Exploring the diversity of Asian Cryptocercus (Blattodea : Cryptocercidae): species delimitation based on chromosome numbers, morphology and molecular analysis

Authors: Bai, Qikun, Wang, Lili, Wang, Zongqing, Lo, Nathan, and Che, Yanli

Source: Invertebrate Systematics, 32(1) : 69-91

Published By: CSIRO Publishing

URL: https://doi.org/10.1071/IS17003

CSIRO PUBLISHING

Invertebrate Systematics, 2018, **32**, 69–91
https://doi.org/10.1071/IS17003

Exploring the diversity of Asian *Cryptocercus* (Blattodea : Cryptocercidae): species delimitation based on chromosome numbers, morphology and molecular analysis

Qikun Bai[A], *Lili Wang*[A], *Zongqing Wang*[A], *Nathan Lo*[B] *and Yanli Che*[A,C]

[A]College of Plant Protection, Southwest University, Beibei, Chongqing 400716, P.R. China.
[B]School of Life and Environmental Sciences, The University of Sydney, Sydney, NSW 2006, Australia.
[C]Corresponding author. Email: shirleyche2000@126.com

Abstract. Woodroaches from the genus *Cryptocercus* Scudder, 1862 are known to display low levels of morphological divergence, yet significant genetic divergence and variability in chromosome number. Compared with *Cryptocercus* taxa from North America, the diversity of the genus in Asia has received relatively little attention. We performed morphological and karyotypic examinations of multiple taxa from several previously unsampled mountainous areas of central and south-western China, and identified nine candidate species primarily on the basis of chromosome number. We then investigated diversity across all Asian *Cryptocercus*, through phylogenetic analyses of 135 COI sequences and 74 28S rRNA sequences from individuals of 28 localities, including species delimitation analysis in General Mixed Yule Coalescent (GMYC) and Automatic Barcode Gap Discovery (ABGD). Phylogenetic results indicated that individuals from the same locality constituted well supported clades. The congruence of GMYC and ABGD results were in almost perfect accord, with 28 candidate species described on the basis of karyotypes (including the nine identified in this study). We provide evidence that each valley population in the Hengduan Mountains contains a separate evolving lineage. We conclude that the principal cause of the rich *Cryptocercus* diversity in China has been the uplift of the Qinghai-Tibet Plateau.

Additional keywords: ABGD, biogeography, DNA barcode, GMYC, Hengduan Mountains, woodroach

Received 10 January 2017, accepted 1 June 2017, published online 9 January 2018

Introduction

The genus *Cryptocercus* (Blattodea : Cryptocercidae) is a subsocial group consisting of ~22 described species distributed in eastern Asia and North America (Nalepa *et al*. 1997; Burnside *et al*. 1999; Grandcolas 2000; Wang *et al*. 2015; Che *et al*. 2016). All members of the genus feed on wood, live in temperate regions, and are wingless with a similar punctate external morphology (Nalepa 1984; Park and Choe 2003). Cryptocercidae is well established as the sister group of termites (Lo *et al*. 2000, 2006, 2007; Klass and Meier 2006; Inward *et al*. 2007; Ware *et al*. 2008; Cameron *et al*. 2012).

Morphological studies of Cryptocercidae have a long history dating back to the 19th century (Scudder 1862; Bey-Bienko 1935, 1938; Nalepa *et al*. 1997; Grandcolas 2000; Grandcolas *et al*. 2001, 2005; Wang *et al*. 2015). Leg armature and structure of the abdomen tip were the most commonly used characters to delineate the first three described *Cryptocercus* species (*C. punctulatus*, *C. primarius*, *C. relictus*) (Scudder 1862; Bey-Bienko 1935, 1938). Subsequent studies have employed morphological or morphological and/or molecular sequence, karyotypic and gut symbiont data (Kambhampati *et al*.1996; Nalepa *et al*. 1997; Burnside *et al*. 1999; Grandcolas 2000; Grandcolas *et al*. 2005; Wang *et al*. 2015; Che *et al*. 2016) to describe new species in the group. Despite low levels of morphological variation among some groups of *Cryptocercus* in eastern North America and China, the use of molecular sequence and karyotyping have aided the description of several new species in each of these areas, although the descriptions of species in the former region have been contested (Burnside *et al*. 1999; Aldrich *et al*. 2004; Everaerts *et al*. 2008).

The analysis of single-locus mitochondrial data has proven to be a useful tool for species delineation, with several studies utilising a fragment of the mitochondrial cytochrome oxidase I (COI) gene (Smith *et al*. 2005; Desalle 2006; Hausmann *et al*. 2011). Such 'DNA barcode'-based approaches have been successfully used for several insect groups (Caterino *et al*. 2000; Hebert *et al*. 2003), including cockroaches (Knebelsberger and Miller 2007; Evangelista *et al*. 2014; Che *et al*. 2017). Several species delineation methods using single-locus data have been proposed, including the General Mixed Yule-coalescent (GMYC) (Pons *et al*. 2006; Monaghan *et al*. 2009; Fujisawa and Barraclough 2013) and Automatic Barcode Gap Discovery (ABGD) (Puillandre *et al*. 2012). An advantage of GMYC is

that it allows for statistical inference and hypothesis testing across the entire sampled clade on an ultrametric tree (Fujisawa and Barraclough 2013). ABGD divides the data into groups based on statistically inferred barcode gaps and distinguishes partitions in the genetic distances among a group of individuals. Comparison of the results from these two methods with each other and with those from traditional methods can be performed to assess their robustness.

In recent decades the number of proposed species of *Cryptocercus* from eastern Asia has increased markedly, from two to 16. These species have been described on the basis of morphological characters only, or using morphological and genetic approaches (including karyotype). To date, the use of species delineation methods such as GMYC and ABGD have not been employed. To investigate the diversity of eastern Asian *Cryptocercus*, we performed morphological and karyotypic examinations of multiple taxa from several previously unsampled mountainous areas of central and south-western China, and identified several potentially new candidate species, primarily on the basis of chromosome number. Following this, we generated new COI and 28S rRNA sequences data from a wide variety of representatives of this group, and performed phylogenetic analyses, including GMYC and ABGD. We selected numerous, biogeographically variable localities (Manchuria, Qin-Daba Mountains and Hengduan Mountains) to infer species diversity and examine the evolution of this group in China.

Materials and methods

Taxon sampling

Samples were collected from rotting logs at 28 localities in China (Fig. 1), from three main regions: Hengduan Mountains, Qin-Daba Mountains and Manchuria (Table 1). Collections were limited to single-day-trip trekking in one valley, meaning that deep valleys were difficult to reach and usually not sampled. Specimens were preserved in analytical pure ethanol and stored at −80°C until processing. All specimens are deposited in the institute of Entomology, College of Plant Protection, Southwest University, Chongqing, China.

Morphological analyses

The terminology for morphological structures follows McKittrick (1964), Li *et al.* (2013) and Wang *et al.* (2015).

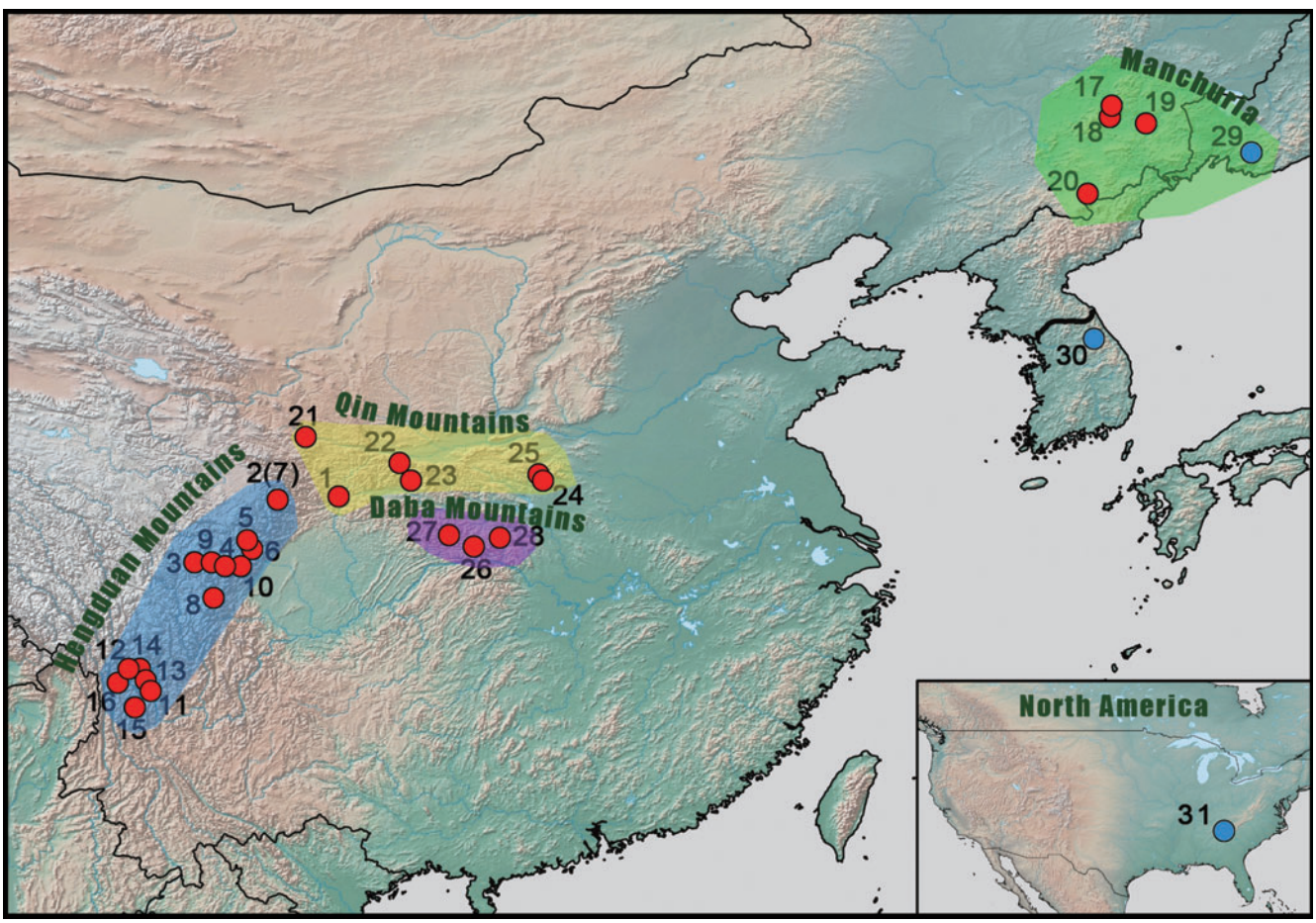

Fig. 1. Map of sampled localities for *Cryptocercus*. Numbers for sampling localities match those in Table 1 (red circles denote samples collected by our team, blue circles denote data obtained from GenBank). The map was generated by www.simplemappr.net using GPS coordinates.

Table 1. Samples used in species delimitation: number of location, sample collection localities, abbreviation of location, and GenBank accession numbers

All localities are in China unless otherwise indicated. The letter 'n' after the voucher abbreviation means the sample is a nymph and the letter 'f' means the sample is female. n.a., not available

Species	Number	Location	Abbreviation	GenBank accession number	
				COI	28S rRNA
C. primarius	1	Qiujiaba (32°59′N, 105°52′E, 2000 m), Longnan City, Gansu Province	QJB1 (f)	KY940647	KU312257
			QJB2 (f)	KY940648	KU312258
C. primarius	2	Dacaoping (32°54′N, 104°03′E, 2993 m), Pingwu County, Mianyang City, Sichuan Province	DCP1	KY940649	KU312232
			DCP2 (n)	KY940650	KU312233
C. matilei	3	Bianerxiang (31°02′N, 101°33′E, 2582 m), Danba County, Sichuan Province	BEX (f)	KY940645	KU312255
			BEX (f)	KY940646	KU312256
C. convexus	4	Bo'ergou (30°51′N, 102°32′E, 3022 m), Jiajinshan, Baoxing County, Ya'an City, Sichuan Province	BRG1 (f)	KY940623	KU312241
			BRG2 (f)	KY940624	KU312242
			BRG3	KY940625	n.a.
			BRG4 (n)	KY940626	n.a.
C. shangmengensis	5	Laojungou (31°40′N, 103°07′E, 2586 m), Lixian County, Sichuan Province	LJG1 (n)	KY940581	KU312224
			LJG2	KY940582	KU312225
			LJG3 (f)	KY940583	n.a.
C. zagunaoensis	6	Danzamugou (31°24′N, 103°15′E, 2912 m), Lixian County, Sichuan Province	DZMG1	KY940584	KU312226
			DZMG2 (f)	KY940585	KU312227
			DZMG3	KY940586	n.a.
C. pingwuensis	7	Baishagou (32°52′N, 104°02′E, 3065 m), Pingwu County, Mianyang City, Sichuan Province	BSG1	KY940612	KU312234
			BSG2 (f)	KY940613	KU312235
C. tianbaensis, sp. nov.	8	Mujiaogou (29°55′N, 102°09′E, 2124 m), Luding County, Sichuan Province	MJG1 (n)	KY940587	KY944598
			MJG2	KY940588	KY944599
			MJG3 (f)	KY940589	n.a.
C. banshanmenensis, sp. nov.	9	Banshanmengou (30°59′N, 102°05′E, 2666 m), Danba County, Sichuan Province	BSM1 (n)	KY940590	KY944600
			BSM2 (n)	KY940591	KY944601
			BSM3	KY940592	n.a.
			BSM4 (f)	KY940593	n.a.
C. wolongensis, sp. nov.	10	Dengsheng (30°51′N, 102°58′E, 2833 m),Wolong County, Sichuan Province	DS1 (n)	KY940594	KY944602
			DS2 (n)	KY940595	KY944603
			DS3	KY940596	n.a.
			DS4 (f)	KY940597	n.a.
C. meridianus	11	Yunshanping (27°08′N, 100°14′E, 3250 m), Yulongxueshan, Lijiang City, Yunnan Province	YLXS1	KY940614	KU312236
			YLXS2 (n)	KY940615	KU312237
			YLXS3 (f)	KY940616	n.a.
C. arcuatus	12	Shikaxueshan (27°47′N, 99°36′E, 3756 m), Shangri-la, Diqing City, Yunnan Province	SKXS1	KY940609	KU312230
			SKXS2	KY940610	KU312231
			SKXS3 (n)	KY940611	n.a.
C. habaensis	13	Habaxueshan (27°22′N, 100°08′E, 3126 m), Shangri-la, Diqing City, Yunnan Province	HBXS1 (f)	KY940578	KU312222
			HBXS2	KY940579	KU312223
			HBXS3 (n)	KY940580	n.a.
C. pudacuoensis, sp. nov.	14	Pudacuo (27°48′N, 99°55′E, 3313 m), Shangri-la, Diqing City, Yunnan Province	PDC1	KY940575	KY944596
			PDC2 (f)	KY940576	KY944597
			PDC3 (n)	KY940577	n.a.
C. laojunensis, sp. nov.	15	Jiushijiulongtan (26°38′N, 99°45′E, 3627 m), Lijiang City, Yunnan Province	JSJLT1 (f)	KY940572	KY944594
			JSJLT2	KY940573	KY944595
			JSJLT3 (n)	KY940574	n.a.
C. weixiensis, sp. nov.	16	Chuandacun (27°21′N, 99°18′E, 2934 m), Weixi County, Yunan Province	CDC1 (f)	KY940651	KY944606
			CDC2 (n)	KY940652	KY944607
			CDC3	KY940653	n.a.
C. relictus	17	Gaolingzi (44°51′N, 128°51′E, 702 m), Shangzhi City, Heilongjiang Province	GLZ1 (n)	KY940640	KU312249
			GLZ2	KY940641	KU312250
C. relictus	18	Shuangfenglinchang (44°32′N, 128°51′E, 1090 m), Hailin City, Heilongjiang Province	SFLC1	KY940636	KU312247
			SFLC2	KY940637	KU312248
			SFLC3 (f)	KY940638	n.a.
			SFLC4 (n)	KY940639	n.a.
C. relictus	19	Mudanfeng (44°20′N, 129°53′E, 1199 m), Mudanjiang City,	MDF1	KY940642	KU312253

(*continued next page*)

Table 1. (*continued*)

Species	Number	Location	Abbreviation	GenBank accession number	
				COI	28S rRNA
		Heilongjiang Province	MDF2	KY940643	KU312254
			MDF3 (n)	KY940644	n.a.
C. changbaiensis, sp. nov.	20	Changbaishan (42°11′N, 128°09′E, 750 m), Jilin Province	CBS1 (f)	KY940654	KY944608
			CBS2	KY940655	KY944609
C. hirtus	21	Shimen Mountain (34°47′N, 104°53′E, 1850 m), Tianshui City, Gansu Province	SMM1 (n)	KY940620	KU312240
			SMM2 (n)	KY940621	n.a.
			SMM3 (n)	KY940622	n.a.
C. hirtus	22	Yangpigou (34°01′N, 107°41′E, 2600 m), Taibai Mountain, Taibai County, Shaanxi Province	YPG1 (f)	KY940633	KU312251
			YPG2 (f)	KY940634	KU312252
			YPG3	KY940635	n.a.
C. ningshanensis	23	Luoboyugou, Tianhua Mountain (33°30′N, 108°02′E, 2000 m), Ningshan County, Shaanxi Province	LBYG1 (n)	KY940629	KU312245
			LBYG2 (n)	KY940630	KU312246
			LBYG3 (n)	KY940631	n.a.
			LBYG4 (f)	KY940632	n.a.
C. neixiangensis	24	Baotianman (33°30′N, 111°56′E, 1470 m), Neixiang County, Nanyang City, Henan Province	BTM1	KY940598	KU312228
			BTM2 (f)	KY940599	KU312229
			BTM3 (n)	KY940600	n.a.
C. luanchuanensis, sp. nov.	25	Longyuwan (33°40′N, 111°48′E,1718 m), Luanchuan County, Henan Province	LYW1 (n)	KY940601	KY944604
			LYW2	KY940602	KY944605
			LYW3	KY940603	n.a.
			LYW4	KY940604	n.a.
			LYW5	KY940605	n.a.
C. wuxiensis	26	Yintiaoling (31°28′N, 109°53′E, 1500 m), Baiguolinchang, Wuxi County, Chongqing	YTL1	KY940617	KU312238
			YTL2 (f)	KY940618	KU312239
			YTL3 (n)	KY940619	n.a.
C. chengkouensis, sp. nov.	27	Xinglongcun (31°51′N, 109°08′E, 1621 m), Chengkou County, Chongqing	XLC1	KY940606	KY944610
			XLC2 (f)	KY940607	KY944611
			XLC3 (f)	KY940608	n.a.
C. shennongjiaensis	28	Songbai Town (31°45′N, 110°40′E, 1750 m), Shennongjia, Hubei Province	HPT1 (f)	KY940627	KU312243
			HPT2 (n)	KY940628	KU312244
C. relictus	29	Anisimovka, Siberia, Russia	ASR	NC018132	n.a.
C. kyebangensis	30	Gangwon Province, South Korea	GPSK	KP986401	KP986242
C. relictus		Russia	BL119	FJ802747	n.a.
C. darwini	31	Cheaha State Park, Alabama, US	CSP1 (f)	KY940656	KY944612
			CSP2	KY940657	KY944613
Cryptocercus sp. 1		North America	USA1	KP986402	n.a.
Cryptocercus sp. 2		North America	USA2	AY165647	n.a.

We identified the species based on five standard characters of female genitalia (anterior margin of Tergite VII, shape of the spermatheca, shape of the basivalvulae, shape and coloration of the laterosternal shelf, length of the paraprocts), which are stable and can be used to distinguish species to a certain extent (Grandcolas 2000; Grandcolas *et al*. 2001, 2005; Aldrich *et al*. 2004; Wang *et al*. 2015). We use abbreviations to indicate the following structures: paraprocts (pp.), first to third valve (v.I, v.II, v.III), paratergites (pt.), anterior arch (a.a.), basivalvula (bsv.), laterosternite IX (ltst.IX), laterosternal shelf (ltst.sh), vestibular sclerite (vst.s.), intersternal fold (inst.f.), central apodeme (c.a.) and spermatheca (sp.). Preparation of genitalia followed the standard procedure, using 10% NaOH to clear internal tissues, then all genitalia were mounted on microscope slides using a Motic K400 stereomicroscope. Photographs of the female genitalia were made using a Leica M205A microscope with a Leica DFC camera. Adults were photographed with a digital camera (Canon 50D) with the aid of the Helicon Focus software.

Karyotype analysis

For karyotype analysis, three individuals from three different logs within each population were examined. Mitotic chromosomes from the testes of males were examined following Luykx (1983). Karyotypes are reported as the diploid complement.

DNA extraction and sequencing

Genomic DNA was extracted from legs by using the TIANamp Genomic DNA Kit (DP304, TIANGEN). Primers are provided in Table S1, available as supplementary material to this paper. All the reactions were carried out in volumes of 25 μL, containing 14.25 μL of ultrapure water, 2.5 μL of 10 × buffer (Mg^{2+} free), 2 μL of $MgCl_2$ (25 mM), 2 μL of dNTP mixture, 1 μL of each primer, 0.25 μL of Taq polymerase, and 2 μL of DNA template. The following steps were performed on a programmable thermal cycler. The amplification protocol setting used were 94°C for 5 min; followed by 35 cycles at 94°C for 45s, 48°C for 45s, and

72°C for 45s; and final extension at 72°C for 10 min. PCR reactions were separated by electrophoresis on a 1% agarose gel. All DNA purification and sequencing was carried out by BGI Tech (Beijing, China) using the aforementioned primers. All sequences were deposited in GenBank, at the National Center for Biotechnology Information (Table 1).

Sequence analysis

A total of 135 cytochrome *c* oxidase subunit I (COI) sequences were analysed, including: 86 sequences from this study; five sequences representing four species from North America and Korea downloaded from GenBank; and 44 sequences representing termite outgroups (Table S2). To provide a comparison with the results from COI, we also analysed two sequences of 28S rRNA for each species (74 total sequences) (Table 1). COI sequences were aligned using MUSCLE 3.8 (Edgar 2004) and adjusted visually and manually corrected after translation into amino acid sequences; 28S rRNA sequences were inspected visually and manually. Intraspecific and interspecific genetic divergence values were quantified based on the Kimura 2-parameter (K2P) distance model (Kimura 1980), using MEGA 6.0.6 (Tamura *et al*. 2013), with 1000 bootstrap replicates.

To explore phylogenetic relationship among these closely related species, phylogenetic trees were constructed on two different datasets (single COI dataset and the concatenated dataset) using Maximum Likelihood (ML) and Bayesian Inference (BI). Bayesian analysis was implemented in MrBayes 3.2 (Ronquist *et al*. 2012), assigning site-specific models. The COI dataset was divided into three partitions by codon position (pos1–3), and PartitionFinder 1.1.1 (Lanfear *et al*. 2012) was used to determine the best-fitting models for each partition. The best-fitting models were as follows: COI_pos1, TVM+G; COI_pos2, TrNef+G; COI_pos3, TrN+I+G; 28S rRNA, TrN+I+G. Two independent sets of Markov chains were run, each with one cold and three heated chains for 1×10^7 generations, and every 1000th generation was sampled. Convergence was inferred when a standard deviation of split frequencies <0.01 was completed. Sump and sumt burninfrac was set to 25% and contype was set to allcompat. Maximum likelihood was implemented in RAxML 7.3.0 (Stamatakis *et al*. 2008); as the software does not allow different substitution models for different partitions we used the GTRGAMMA model for analyses. Bootstrap values were performed for 1000 replicates.

All COI sequences were analysed using ABGD and GMYC. ABGD analysis was performed using a web interface (http://wwwabi.snv.jussieu.fr/public/abgd/, accessed 4 May 2017); the default parameters were used except for the relative gap width, which was set as 1.0. The GMYC method requires a fully resolved ultrametric tree as input for the analysis. We constructed a Bayesian inference tree in BEAST 1.8.1 (Drummond and Rambaut 2007) using the best-fitting models from PartitionFinder. Rate variation was modelled among branches using an uncorrelated log-normal relaxed clock model with the mean clock rate fixed to 1.0. A UPGMA starting tree was used in the analysis, and the constant size coalescent was used as a prior on divergence times. We performed two replicate MCMC runs, and sampled every 5000 steps over a total of 50 million generations. A maximum clade credibility tree was obtained using Tree Annotator within the BEAST software package with a burn-in of 1000 trees. We then applied the single-threshold GMYC method to the ultrametric gene tree generated by BEAST using the SPLITS package (Ezard *et al*. 2009) in R software (R Core Team 2013). The groups delimited were compared with a one-species null model using a likelihood ratio test.

Results

Karyotypes and taxonomy of novel Cryptocercus species

Through examination of the morphology and chromosome numbers of cockroaches from previously unsampled areas, we identified nine new candidate *Cryptocercus* species: *C. changbaiensis*, sp. nov.; *C. weixiensis*, sp. nov.; *C. luanchuanensis*, sp. nov. ($2n = 39$) (Fig. 2*H*); *C. chengkouensis*, sp. nov. ($2n = 29$) (Fig. 2*A*); *C. wolongensis*, sp. nov. ($2n = 43$) (Fig. 2*B*); *C. banshanmenensis*, sp. nov. ($2n = 29$) (Fig. 2*C*); *C. tianbaensis*, sp. nov. ($2n = 35$) (Fig. 2*D*); *C. laojunensis*, sp. nov. ($2n = 21$) (Fig. 2*E*); *C. pudacuoensis*, sp. nov. ($2n = 21$) (Fig. 2*F*). All species of Chinese *Cryptocercus* examined in this study were highly similar in external morphology, including female genitalia (see Table 2, e.g. *C. luanchuanensis*, sp. nov. and *C. neixiangensis*). All candidate new species are named after their type localities.

COI and 28S rRNA sequence variation across Asian taxa

We next obtained molecular sequence data from mitochondrial COI and 28S rRNA from multiple Asian taxa. The sequenced lengths of COI and 28S rRNA, excluding primers, were ~658 bp and 635 bp respectively. All new sequences have been deposited in GenBank with accession numbers KY940572 to KY940657 for COI (accession numbers for 28S in Table 1). Among aligned COI sequences 232 sites were variable, of which 217 were parsimony informative. Among aligned 28S rRNA sequences, 106 sites were variable, of which 103 were parsimony informative.

Intraspecific COI genetic divergence (K2P) ranged from 0.00 to 0.61%, with an average of 0.14%. The greatest intraspecific COI genetic divergence (0.61%) occurred in *C. darwini*. All intraspecific COI genetic divergence values were less than 0.5%, and many intraspecific COI genetic divergence values were 0.00% (Table S3). Interspecific COI genetic divergence ranged from 2.18% (*C. neixiangensis* and *C. luanchuanensis*, sp. nov.) to 20.36% (*C. chengkouensis*, sp. nov. and *C. darwini*), with an average of 11.81% (Table S3). The 28S sequences of *Cryptocercus* had low levels of genetic divergence of 96.27% and lacked sufficient variation to resolve some species (Table S4). 28 species were identified through the use of the barcoding gap, of which nine were new (Fig. 3*B*).

GMYC, ABGD, and other phylogenetic analyses

The likelihoods of the null and GMYC models from COI analysis were 239.49 and 268.42 respectively. The GMYC was an improvement over the null model, and was clustered into 72 (confidence interval: 72–73) entities (likelihood ratio = 57.87) including 28 *Cryptocercus* and 44 termite species. ABGD

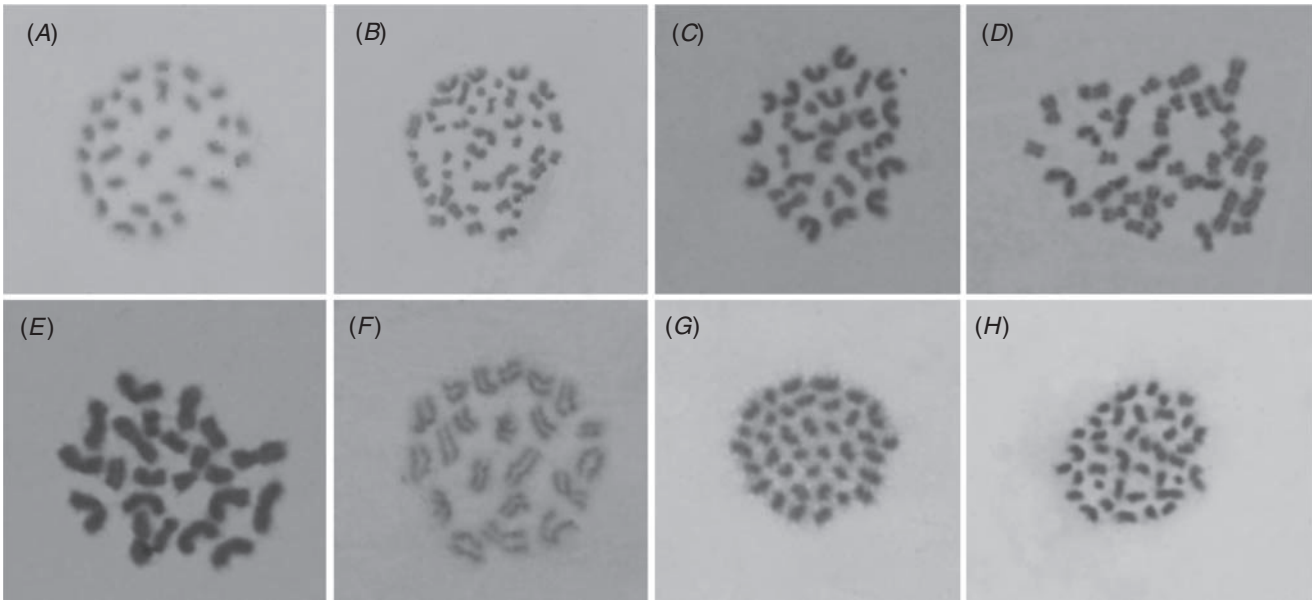

Fig. 2. Mitotic chromosomes of males of *Cryptocercus* species. (*A*) *C. chengkouensis*, sp. nov. (XLC) (2*n* = 29); (*B*) *C. wolongensis*, sp. nov. (DS) (2*n* = 43); (*C*) *C. banshanmenensis*, sp. nov. (BSM) (2*n* = 29); (*D*) *C. tianbaensis*, sp. nov. (MJG) (2*n* = 35); (*E*) *C. laojunensis*, sp. nov. (JSJLT) (2*n* = 21); (*F*) *C. pudacuoensis*, sp. nov. (PDC) (2*n* = 21); (*G*) *C. neixiangensis* (BTM) (2*n* = 37); (*H*) *C. luanchuanensis*, sp. nov. (LYW) (2*n* = 39).

based on the same dataset also detected 72 species with a range of prior intraspecific values ($P = 0.0046$–0.0215) (Fig. 3*C*).

Phylogenetic analyses performed using ML and BI recovered similar tree topologies in COI analysis with some differences in branching patterns at deeper nodes. Support values from ML analysis were much higher than those from BI analysis (Figs 3, S1). Representatives from candidate species (described primarily on the basis of karyotype number) were found to form monophyletic groups. Analyses based on concatenated COI and 28S sequences revealed similar topologies to those inferred from COI only, with some minor differences.

Asian and American lineages (α and β) formed monophyletic groups, as recovered in BI and ML analyses for COI and combined datasets (Figs 3, S1, S2). For COI analysis (Fig. 3), all species from Qin-Dada Mountains were clustered together with strong support (Clade γ). Species from Manchuria and the Hengduan Mountains were clustered together (Clade δ) with one exception (*C. pudacuoensis*, sp. nov. (PDC)), although this grouping was not well supported.

Taxonomy

Genus ***Cryptocercus*** Scudder

Cryptocercus Scudder 1862: 419. – Bey-Bienko 1935: 130; Bey-Bienko 1938: 237; Nalepa *et al.* 1997: 416; Burnside *et al.* 1999: 361; Grandcolas 2000: 223; Grandcolas *et al.* 2001: 61; Aldrich *et al.* 2004: 443; Grandcolas *et al.* 2005: 725; Wang *et al.* 2015: 260; Che *et al.* 2016: 201.

Cryptocercus chengkouensis, sp. nov.

(Figs 4*a*1–4*a*3, 5)

http://zoobank.org/urn:lsid:zoobank.org:act: CD5EBB2A-9636-4DFE-AA92-7C36327837B8

Material examined

Holotype. ♀, China: Chongqing City, Chengkou County, Xinglongcun, 1621 m, 30.x.2014, coll. Xinran Li and Yan Shi.

Paratypes. 2♂, 1♀, same data as holotype.

Measurements

Male and female – pronotum, length × width: 6.5 × 8.5 mm; body length: 25.5–27.5 mm.

Description

Tergite VII with anterior margin slightly arched and posterior margin rounded (Fig. 5*D*). Sternum VII slightly produced at apex, posterior margin truncate (Fig. 5*C*). Tergite X rounded at apex; paraprocts (pp.) developed, triangular, with apices extending to the posterior margin of Tergite X (this sample was broken at apex) (Fig. 5*A*).

Female genitalia

Basivalvulae (bsv.) well-developed and divided into two symmetrical parts; basivalvulae with anterior and posterior margins clearly delimited, posterior margins obscure and dark brown, anterior area dark brown with a distinctive prominence (Fig. 5*E*). Spermatheca sitting behind the basivalvulae and with a large and oval apical ampulla, and an oval basal ampulla on a short duct. Laterosternal shelf (ltst.sh.) large and translucent, nearly oval and brown on both sides, with dense spinules at apical half (Fig. 5*F*).

Cryptocercus changbaiensis, sp. nov.

(Figs 4*b*1–4*b*3, 6)

http://zoobank.org/urn:lsid:zoobank.org:act:DEA5D9D6-FB94-4C8F-B9A4-18C454C09C4C

Table 2. Comparison of female genitalia of 21 Chinese *Cryptocercus* species

Species	Standard characters of female genitalia that were used in this study				
	Anterior margin of Tergite VII	Shape of spermatheca	Shape of basivalvulae	Shape and coloration of laterosternal shelf	Length of paraprocts
Manchuria					
C. changbaiensis, sp. nov.	Slightly arched	Round	Anterior area narrow and dark brown	Nearly oval	Do not extend to the posterior margin of Tergite X
C. relictus	Slightly truncate	Round	Anterior area wide and dark brown	Nearly oblong and slightly brown on both sides	Extend to the posterior margin of Tergite X
Qin-Daba Mountains					
C. hirtus	Slightly truncate	Spindle	Anterior area dark brown with a distinctive prominence	Nearly oblong and brown on both sides	Extend to the posterior margin of Tergite X
C. ningshanensis	Slightly arched	Oblong	Anterior area dark brown with a distinctive prominence	Nearly oval and brown on most of both sides	Do not extend to the posterior margin of Tergite X
C. neixiangensis	Slightly arched	Oblong	Anterior area dark brown with a distinctive prominence	Nearly oval and brown on both sides	Do not extend to the posterior margin of Tergite X
C. luanchuanensis, sp. nov.	Truncate and weakly concave at middle	Oblong	Anterior area dark brown with a distinctive prominence	Nearly oval and brown on both sides	Do not extend to the posterior margin of Tergite X
C. shennongjiaensis	Slightly arched	Oval	Anterior area dark brown with a distinctive prominence	Nearly oblong and narrow, brown on both sides	Do not extend to the posterior margin of Tergite X
C. wuxiensis	Slightly arched	Oval	Anterior area dark brown with a distinctive prominence	Nearly oblong and brown on both sides	Do not extend to the posterior margin of Tergite X
C. chengkouensis, sp. nov.	Slightly arched	Oval	Anterior area dark brown with a distinctive prominence	Nearly oval and brown on both sides	Extend to the posterior margin of Tergite X
Hengduan Mountains					
C. meridianus	Distinctly truncate	Round	Anterior area narrow and dark brown	Nearly oblong and brown on most of both sides	Extend to the posterior margin of Tergite X
C. arcuatus	Slightly truncate	Water-drop	Anterior area wide and dark brown	Nearly oblong	Do not extend to the posterior margin of Tergite X
C. pudacuoensis, sp. nov.	Distinctly truncate	Round	Anterior area wide and dark brown	Nearly oval, with dense spinules at apex	Do not extend to the posterior margin of Tergite X
C. habaensis	Slightly truncate	Round	Anterior area narrow and dark brown	Nearly oblong	Do not t extend to the posterior margin of Tergite X
C. laojunensis, sp. nov.	Truncate and weakly concave at middle	Round	Anterior area narrow and dark brown	Nearly oblong and brown on most of both sides	Do not extend to the posterior margin of Tergite X
C. weixiensis, sp. nov.	Slightly arched	Oval	Anterior area narrow and dark brown	Nearly oval and light brown at middle	Do not extend to the posterior margin of Tergite X
C. primarius	Distinctly truncate	Round	Anterior area narrow and dark brown	Nearly oblong	Do not extend to the posterior margin of Tergite X
C. pingwuensis	Slightly truncate	Oblong	Anterior area narrow and dark brown	Nearly oblong	Do not extend to the posterior margin of Tergite X
C. tianbaensis, sp. nov.	Slightly truncate	Oblong	Anterior area wide and dark brown	Nearly oblong and narrow brown at middle	Do not extend to the posterior margin of Tergite X

(*continued next page*)

Table 2. (*continued*)

Species	Standard characters of female genitalia that were used in this study				
	Anterior margin of Tergite VII	Shape of spermatheca	Shape of basivalvulae	Shape and coloration of laterosternal shelf	Length of paraprocts
C. wolongensis, sp. nov.	Slightly truncate	Water-drop	Anterior area narrow and dark brown	Nearly oval and light brown at middle	Do not extend to the posterior margin of Tergite X
C. convexus	Truncate and weakly concave at middle	Round	Anterior area narrow and dark brown	Nearly oval and light brown at middle	Do not extend to the posterior margin of Tergite X
C. banshanmenensis, sp. nov.	Slightly truncate and concave	Water-drop	Anterior area narrow and dark brown	Nearly oblong	Do not extend to the posterior margin of Tergite X

Material examined

Holotype. ♀, China: Jilin Prov., Mt Changbai, 750 m, 7.viii.2015, coll. Yejie Lin.

Paratypes. 4♂, 3♀, same data as holotype.

Measurements

Male and female – pronotum, length × width: 5.5 × 7.5 mm; body length: 24.5–25.5 mm.

Description

Tergite VII with anterior margin slightly arched and posterior margin truncate (Fig. 6*D*). Sternum VII strongly produced at apex, posterior margin truncate (Fig. 6*C*). Tergite X finely acute at apex; paraprocts (pp.) developed, triangular, with apices not extending to the posterior margin of Tergite X (Fig. 6*A*).

Female genitalia

Basivalvulae (bsv.) well-developed and divided into two symmetrical parts; basivalvulae with anterior and posterior margins clearly delimited, posterior margins obscure and dark brown, anterior area narrow and dark brown (Fig. 6*E*). Spermatheca sitting behind the basivalvulae and with a large and round apical ampulla, and a round basal ampulla on a short duct. Laterosternal shelf (ltst.sh.) large and translucent, nearly oval, with dense spinules at apex (Fig. 6*F*).

Cryptocercus wolongensis, sp. nov.

(Figs 4*c*1–4*c*3, 7)

http://zoobank.org/urn:lsid:zoobank.org:act:96ECCA44-4BCB-47A3-93BC-F505F38CEF35

Material examined

Holotype. ♀, China: Sichuan Prov., Wolong County, Dengsheng, 2833 m, 6.x.2014, coll. Yan Shi and Lu Qiu.

Paratypes. 1♂, 5♀, same data as holotype.

Measurements

Male and female – pronotum, length × width: 7.1 × 8.9 mm; body length: 29.9–30.5 mm.

Description

Tergite VII with anterior margin slightly truncate and posterior margin truncate (Fig. 7*D*). Sternum VII produced at apex, posterior margin truncate (Fig. 7*C*); Tergite X rounded at apex; paraprocts (pp.) developed, triangular, with apices not extending to the posterior margin of Tergite X (Fig. 7*A*).

Female genitalia

Basivalvulae (bsv.) well-developed and divided into two symmetrical parts; basivalvulae with anterior and posterior margins clearly delimited, posterior margins obscure and dark brown, anterior area narrow and dark brown (Fig. 7*E*). Spermatheca sitting behind the basivalvulae and with a large and water-drop apical ampulla, and a water-drop basal ampulla on a short duct. Laterosternal shelf (ltst.sh.) large and translucent, nearly oval and light brown at middle, with dense spinules at apical half (Fig. 7*F*).

Cryptocercus weixiensis, sp. nov.

(Figs 4*d*1–4*d*3, 8)

http://zoobank.org/urn:lsid:zoobank.org:act:F1F83000-09D1-4529-9C13-7A633208FB34

Material examined

Holotype. ♀, China: Yunnan Prov., Weixi County, Pantiange, 2934 m, 21.viii.2015, coll. Qikun Bai and Lu Qiu.

Paratypes. 1♂, 2♀, same data as holotype.

Measurements

Male and female – pronotum, length × width: 5.5 × 7.5 mm; body length: 21–22.5 mm.

Description

Tergite VII with anterior margin slightly arched and posterior margin truncate (Fig. 8*D*). Sternum VII produced at apex, posterior margin truncate (Fig. 8*C*). Tergite X rounded at apex; paraprocts (pp.) developed, triangular, with apices not extending to the posterior margin of Tergite X, with the gap between paraprocts narrow (Fig. 8*A*).

Fig. 3. Maximum-likelihood tree based on COI genes (BPP: Bayesian Posterior Probabilities; MLB: Maximum Likelihood Bootstrap Values). A square (■) at a node indicates that both BPP and MLB >95; a circle (●) indicates that only MLB >95. Numbers after the species name are chromosome numbers, numbers in red are results from this study. Coloured bars indicate different species delimitation by different methods: A, morphology; B, DNA barcoding gap; C, GMYC model; D, ABGD result. We selected 86 samples of 28 *Cryptocercus* species. The topology shown was very similar to that produced by the BI tree, with some differences (see Fig. S1).

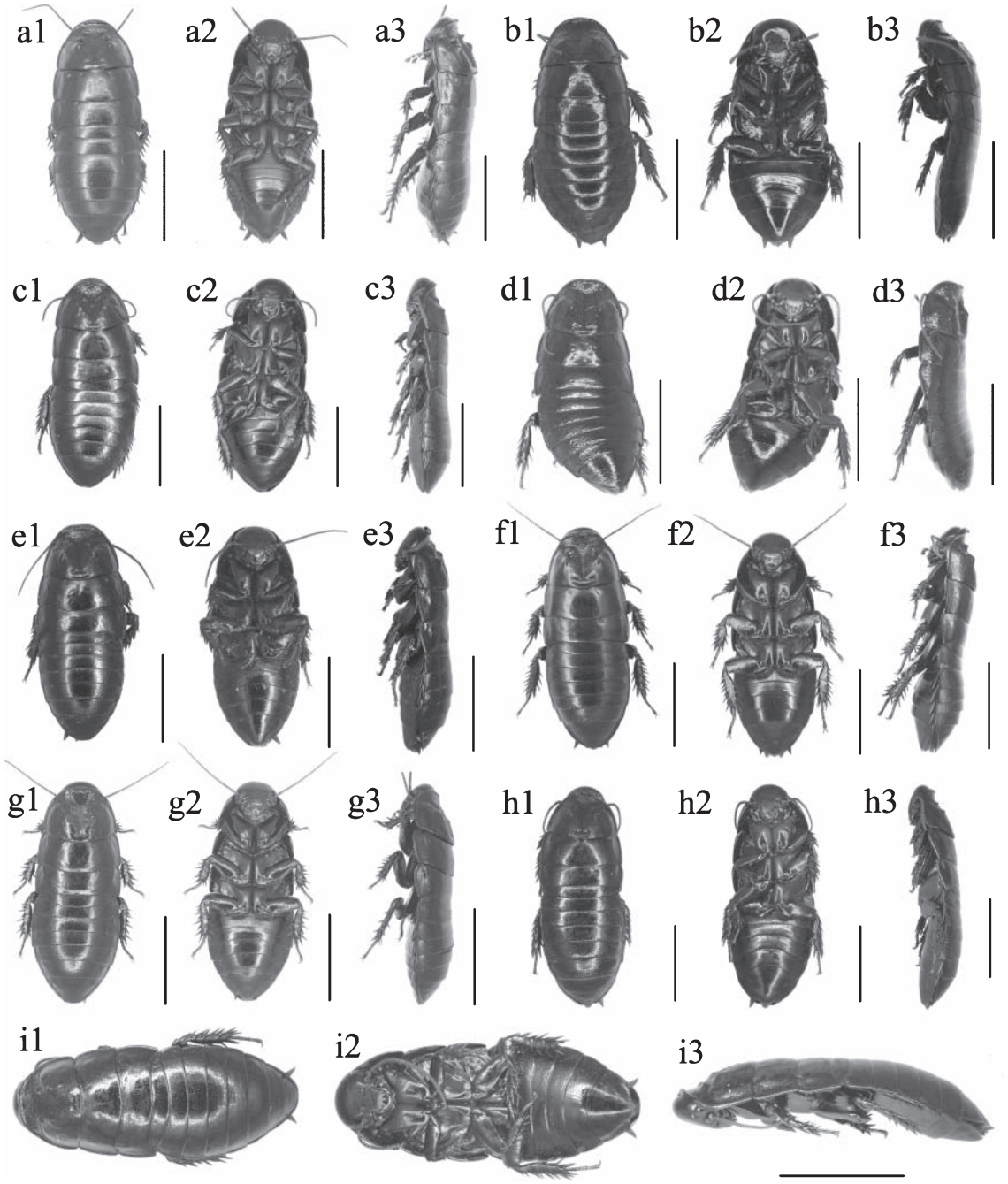

Fig. 4. a1–a3: *Cryptocercus chengkouensis*, sp. nov., holotype: a1, dorsal view; a2, ventral view; a3, lateral view. b1–b3: *Cryptocercus changbaiensis*, sp. nov., holotype: b1, dorsal view; b2, ventral view; b3, lateral view. c1–c3: *Cryptocercus wolongensis*, sp. nov., holotype: c1, dorsal view; c2, ventral view; c3, lateral view. d1–d3: *Cryptocercus weixiensis*, sp. nov., holotype: d1, dorsal view; d2, ventral view; d3, lateral view. e1–e3: *Cryptocercus pudacuoensis*, sp. nov., holotype: e1, dorsal view; e2, ventral view; e3, lateral view. f1–f3: *Cryptocercus luanchuanensis*, sp. nov., holotype: f1, dorsal view; f2, ventral view; f3, lateral view. g1–g3: *Cryptocercus laojunensis*, sp. nov., holotype: g1, dorsal view; g2, ventral view; g3, lateral view. h1–h3: *Cryptocercus banshanmenensis*, sp. nov., paratype: h1, dorsal view; h2, ventral view; h3, lateral view. i1–i3: *Cryptocercus tianbaensis*, sp. nov., paratype: i1, dorsal view; i2, ventral view; i3, lateral view. Scale bars: 1.0 cm.

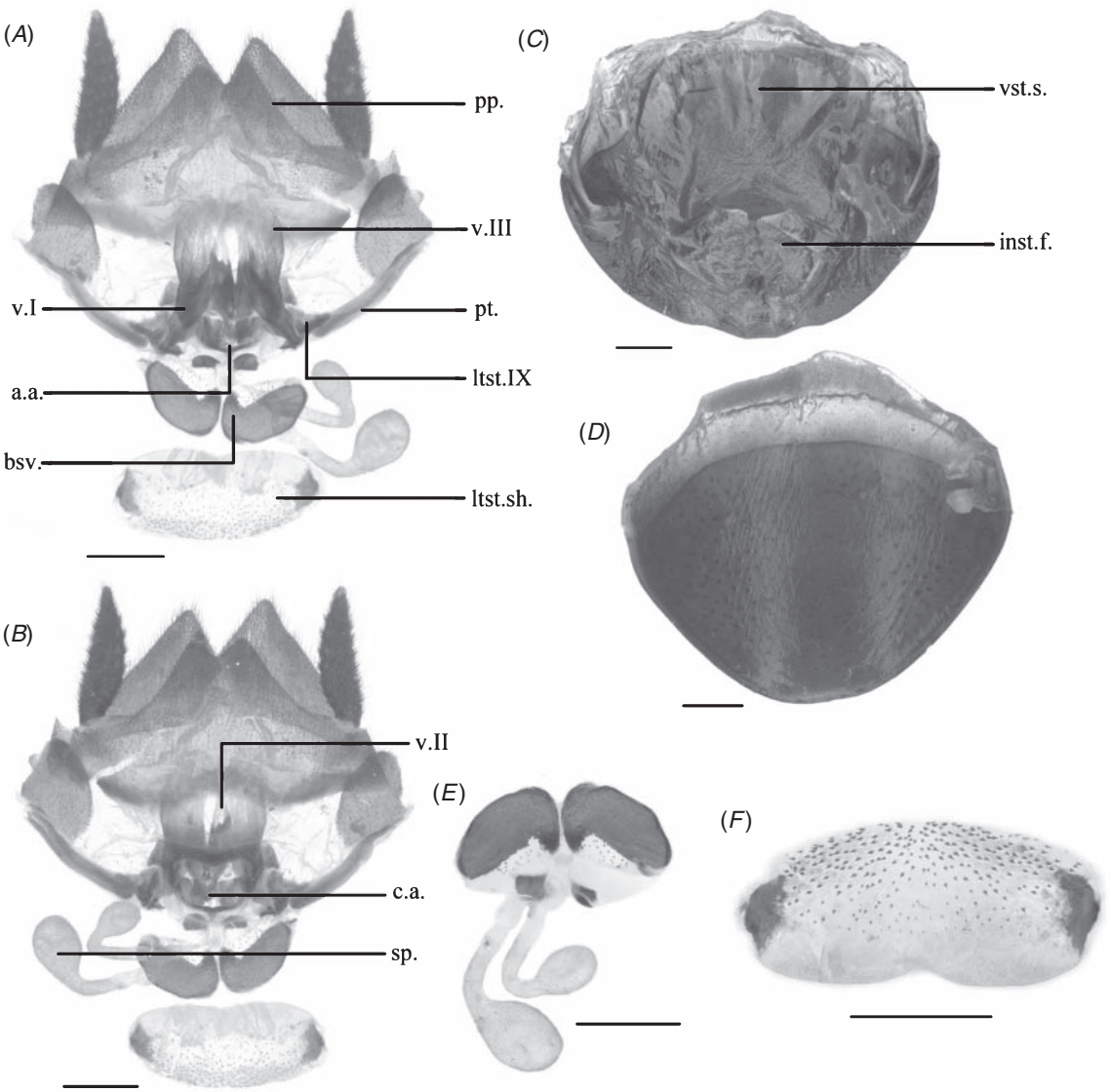

Fig. 5. *Cryptocercus chengkouensis*, sp. nov.: (*A*) supraanal plate, ventral view; (*B*) supraanal plate, dorsal view; (*C*) subgenital plate, dorsal view; (*D*) Tergite VII, dorsal view; (*E*) basivalvula and spermatheca, ventral view; (*F*) laterosternal shelf, dorsal view. Scale bars: 1.0 mm.

Female genitalia

Basivalvulae (bsv.) well-developed and divided into two symmetrical parts; basivalvulae with anterior and posterior margins clearly delimited, posterior margins obscure and dark brown, anterior area narrow and dark brown (Fig. 8*E*). Spermatheca sitting behind the basivalvulae and with a large and oval apical ampulla, and an oval basal ampulla on a short duct. Laterosternal shelf (ltst.sh.) large and translucent, nearly oval and light brown on both sides, with dense spinules at apical half (Fig. 8*F*).

Cryptocercus pudacuoensis, sp. nov.

(Figs 4*e*1–4*e*3, 9)

http://zoobank.org/urn:lsid:zoobank.org:act:63DA3139-7F99-4111-8E75-78E850074630

Material examined

Holotype. ♀, China: Yunnan Prov., Diqing City, Shangri-La Pudacuo, 3313 m, 14.x.2014, coll. Qikun Bai and Yan Shi.

Paratypes. 4♂, 2♀, same data as holotype.

Measurements

Male and female – pronotum, length × width: 6.5 × 8.5 mm; body length: 26.5–27.5 mm.

Description

Tergite VII with anterior margin truncate and posterior margin rounded (Fig. 9*D*). Sternum VII slightly produced at apex, posterior margin truncate (Fig. 9*C*). Tergite X rounded at apex; paraprocts (pp.) developed, triangular, with apices not

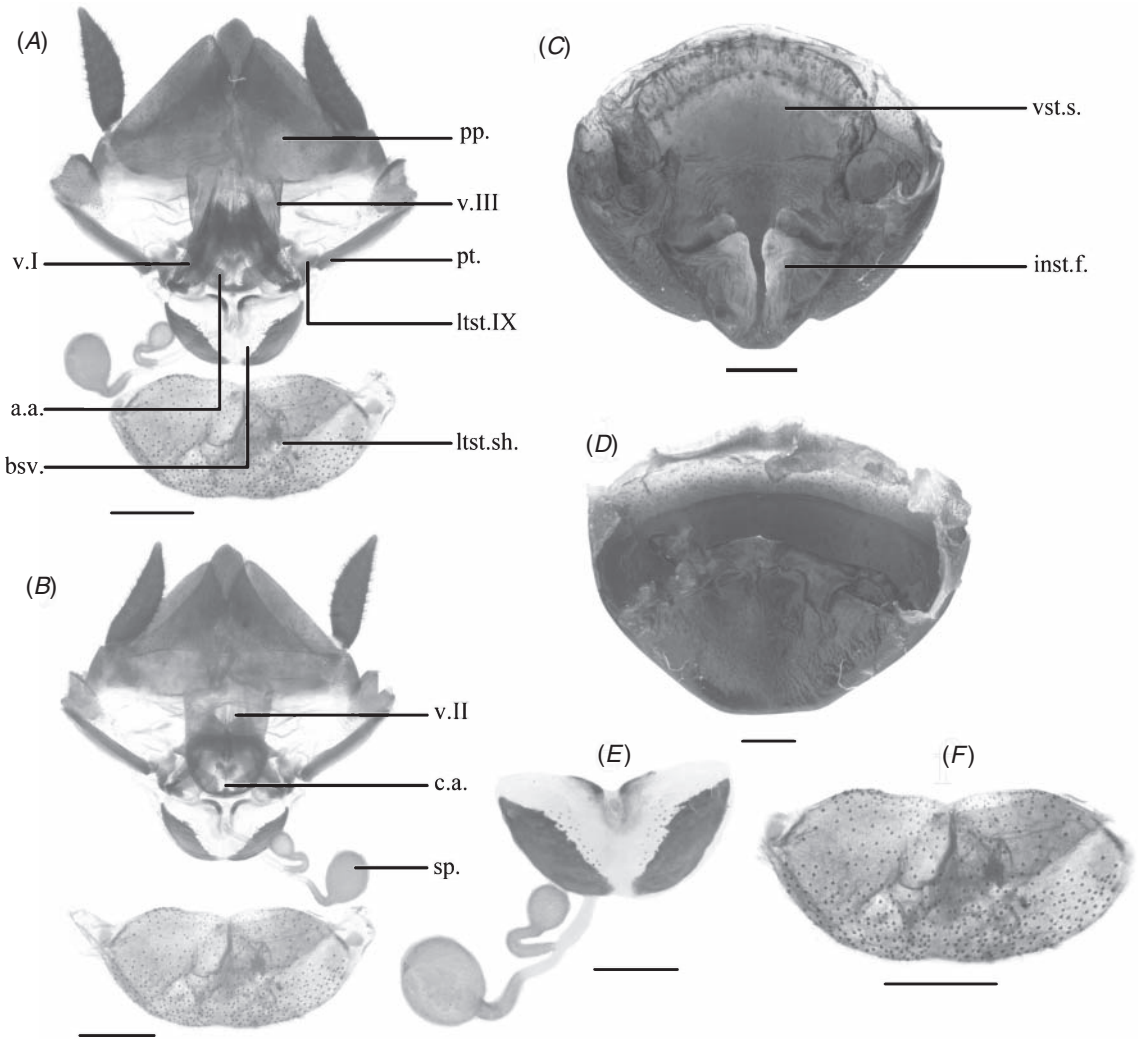

Fig. 6. *Cryptocercus changbaiensis*, sp. nov.: (*A*) supraanal plate, ventral view; (*B*) supraanal plate, dorsal view; (*C*) subgenital plate, dorsal view; (*D*) Tergite VII, dorsal view; (*E*) basivalvula and spermatheca, ventral view; (*F*) laterosternal shelf, dorsal view. Scale bars: 1.0 mm.

extending to the posterior margin of Tergite X, with the gap between paraprocts narrow (Fig. 9*A*).

Female genitalia

Basivalvulae (bsv.) well-developed and divided into two symmetrical parts; basivalvulae with anterior and posterior margins clearly delimited, posterior margins obscure and dark brown, anterior area wide and dark brown (Fig. 9*E*). Spermatheca sitting behind the basivalvulae and with a large and round apical ampulla, and a round basal ampulla on a short duct. Laterosternal shelf (ltst.sh.) large and translucent, nearly oval, with dense spinules at apex (Fig. 9*F*).

Cryptocercus luanchuanensis, sp. nov.

(Figs 4*f*1–4*f*3, 10)

http://zoobank.org/urn:lsid:zoobank.org:act:FF00A947-0C54-47B9-90B3-0A39479E7BA5

Material examined

Holotype. ♀, China: Henan Prov., Luanchuan County, Longyuwan, 1718 m, 26.x.2014, coll. Xinran Li and Yan Shi.

Paratypes. 4♂, 4♀, same data as holotype.

Measurements

Male and female – pronotum, length × width: 5.5 × 8.2 mm; body length: 26.5–27.5 mm.

Description

Tergite VII with anterior margin slightly arched and posterior margin truncate (Fig. 10*D*). Sternum VII slightly produced at apex, posterior margin truncate and weakly concave at middle (Fig. 10*C*). Tergite X rounded at apex; paraprocts (pp.) developed, triangular, with apices not extending to the posterior margin of Tergite X, with the gap between paraprocts narrow (Fig. 10*A*).

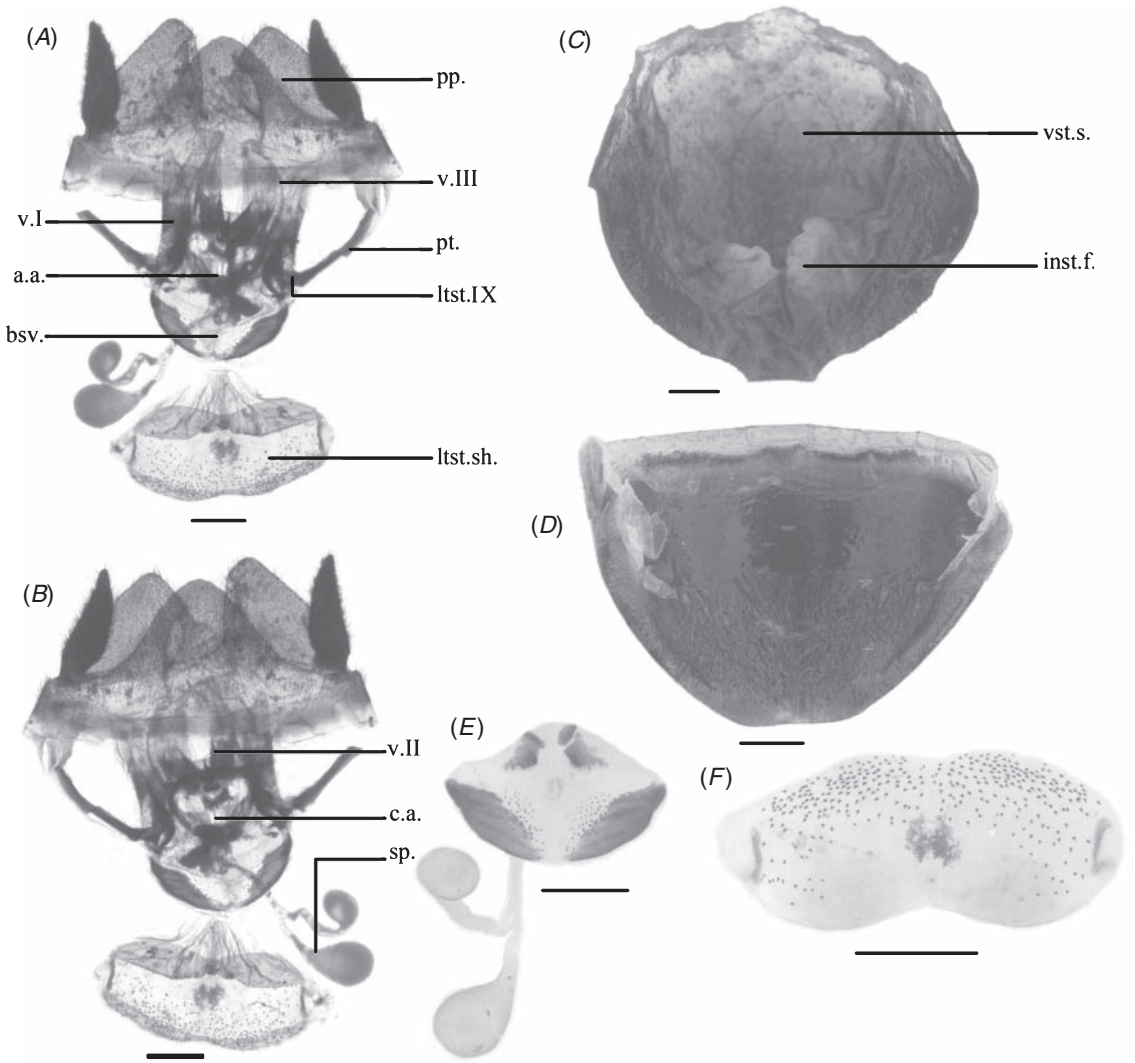

Fig. 7. *Cryptocercus wolongensis*, sp. nov.: (*A*) supraanal plate, ventral view; (*B*) supraanal plate, dorsal view; (*C*) subgenital plate, dorsal view; (*D*) Tergite VII, dorsal view; (*E*) basivalvula and spermatheca, ventral view; (*F*) laterosternal shelf, dorsal view. Scale bars: 1.0 mm.

Female genitalia

Basivalvulae (bsv.) well-developed and divided into two symmetrical parts; basivalvulae with anterior and posterior margins clearly delimited, posterior margins obscure and dark brown, anterior area dark brown with a distinctive prominence (Fig. 10*E*). Spermatheca sitting behind the basivalvulae and with a large and oblong apical ampulla, and an oblong basal ampulla on a short duct. Laterosternal shelf (ltst.sh.) large and translucent, nearly oval and brown on both sides, with dense spinules at apical half (Fig. 10*F*).

Cryptocercus laojunensis, sp. nov.

(Figs 4*g*1–4*g*3, 11)

http://zoobank.org/urn:lsid:zoobank.org:act:D9C3FCF5-A596-4808-A7D3-F43479D6C7A6

Material examined

Holotype. ♀, China: Yunnan Prov., Lijiang City, Mt Laojunshan, Jiushijiulongtan, 3627 m, 12.x.2014, coll. Qikun Bai and Yan Shi.

Paratypes. 3♂, 6♀, same data as holotype.

Measurements

Male and female – pronotum, length × width: 6.1 × 8.0 mm; body length: 23.6 mm.

Description

Tergite VII with anterior margin slightly truncate and posterior margin truncate (Fig. 11*D*). Sternum VII slightly produced at apex, posterior margin truncate and weakly concave at middle. Tergite X rounded at apex (Fig. 11*C*); paraprocts (pp.) developed, triangular, with apices not extending to the posterior margin of Tergite X, with the gap between paraprocts narrow (Fig. 11*A*).

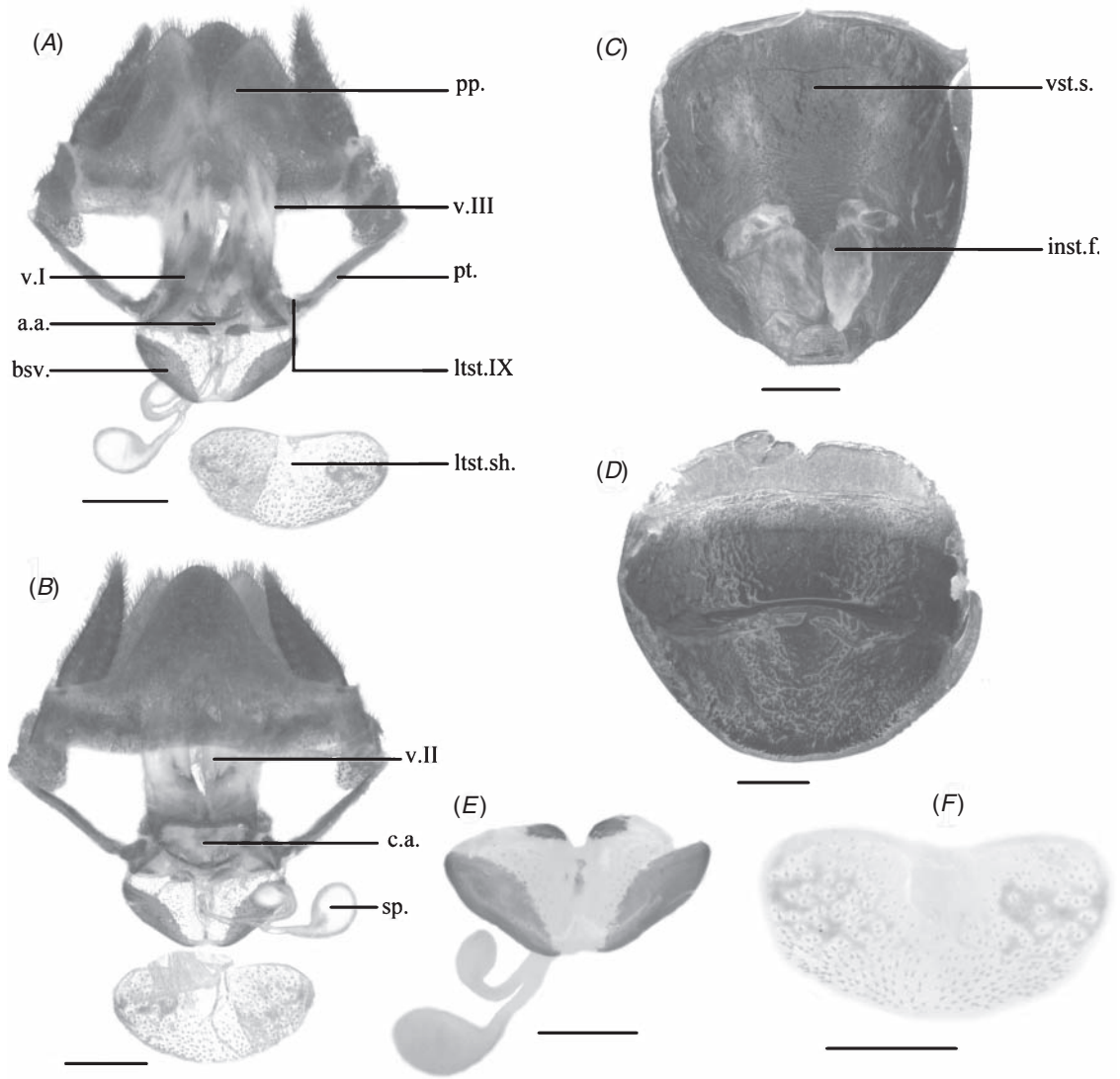

Fig. 8. *Cryptocercus weixiensis*, sp. nov.: (*A*) supraanal plate, ventral view; (*B*) supraanal plate, dorsal view; (*C*) subgenital plate, dorsal view; (*D*) Tergite VII, dorsal view; (*E*) basivalvula and spermatheca, ventral view; (*F*) laterosternal shelf, dorsal view. Scale bars: 1.0 mm.

Female genitalia

Basivalvulae (bsv.) well-developed and divided into two symmetrical parts; basivalvulae with anterior and posterior margins clearly delimited, posterior margins obscure and dark brown, anterior area narrow and dark brown (Fig. 11*E*). Spermatheca sitting behind the basivalvulae and with a large and round apical ampulla, and a very small basal ampulla on a short duct. Laterosternal shelf (ltst.sh.) large and translucent, nearly oblong and brown over much of both sides, with dense spinules at apical half (Fig. 11*F*).

Cryptocercus banshanmenensis, sp. nov.

(Figs 4*h*1–4*h*2, 12)

http://zoobank.org/urn:lsid:zoobank.org:act:D3BDA42D-5321-43D7-A540-2A57E3879609

Material examined

Holotype. ♀, China: Sichuan Prov., Danba County, Banshanmengou, 2666 m, 6.x.2014, coll. Qikun Bai, Zhiwei Qiu and Xinran Li.

Paratypes. 2♂, 2♀, same data as holotype.

Measurements

Male and female – pronotum, length × width: 6.5 × 9.0 mm; body length: 28.5 mm.

Description

Tergite VII with anterior margin slightly truncate and concave, posterior margin truncate (Fig. 12*D*). Sternum VII strongly produced at apex, posterior margin truncate (Fig. 12*C*). Tergite X slightly acute at apex; paraprocts (pp.) developed, triangular, with apices not extending to the posterior margin of Tergite X (Fig. 12*A*).

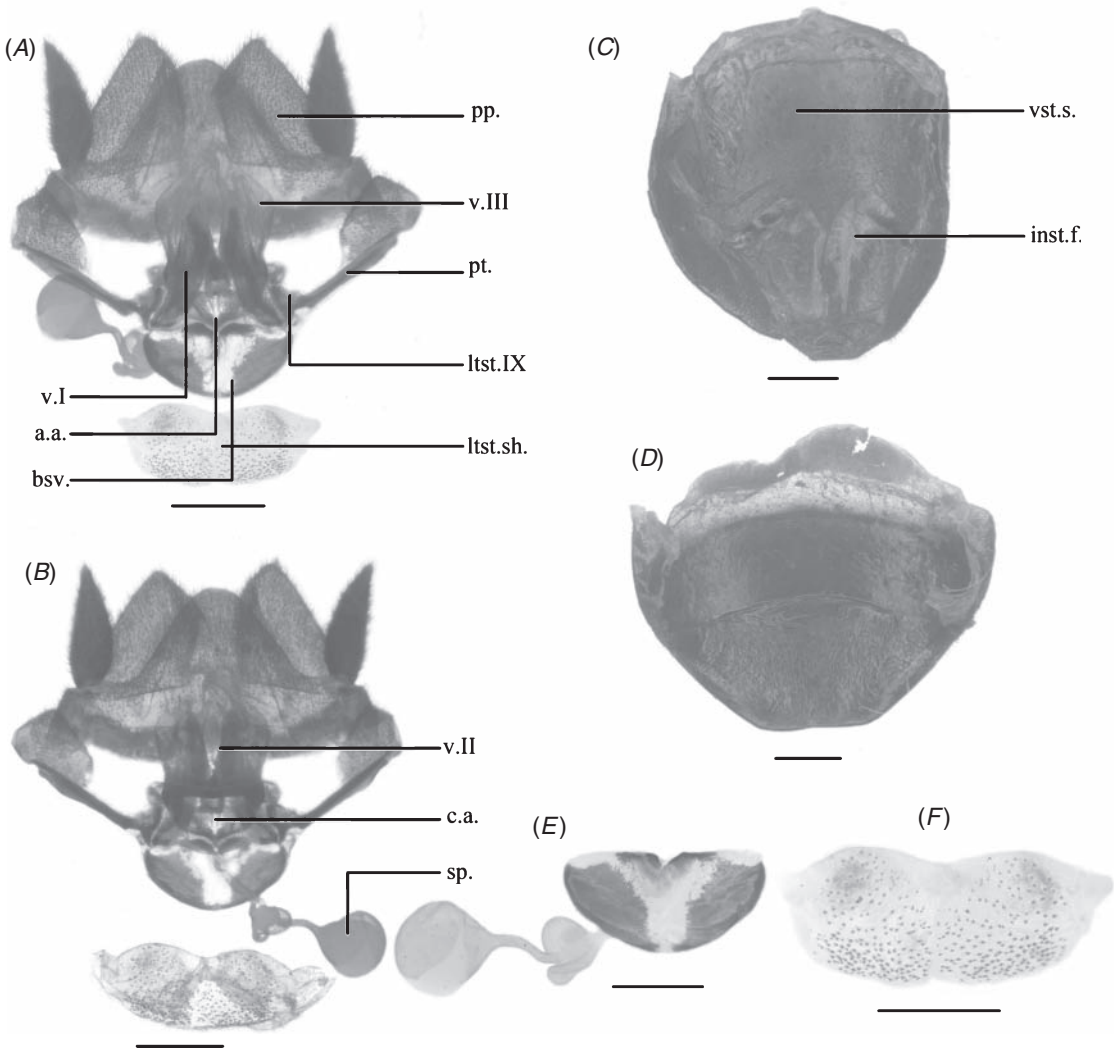

Fig. 9. *Cryptocercus pudacuoensis*, sp. nov.: (*A*) supraanal plate, ventral view; (*B*) supraanal plate, dorsal view; (*C*) subgenital plate, dorsal view; (*D*) Tergite VII, dorsal view; (*E*) basivalvula and spermatheca, ventral view; (*F*) laterosternal shelf, dorsal view. Scale bars: 1.0 mm.

Female genitalia

Basivalvulae (bsv.) well-developed and divided into two symmetrical parts; basivalvulae with anterior and posterior margins clearly delimited, posterior margins obscure and dark brown, anterior area narrow and dark brown (Fig. 12*E*). Spermatheca sitting behind the basivalvulae and with a large and water-drop apical ampulla, and a water-drop basal ampulla on a short duct. Laterosternal shelf (ltst.sh.) large and translucent, nearly oblong, with dense spinules at apical half (Fig. 12*F*).

Cryptocercus tianbaensis, sp. nov.

(Figs 4*i*1–4*i*3, 13)

http://zoobank.org/urn:lsid:zoobank.org:act:919C214E-666B-410B-838A-112D89DF4D97

Material examined

Holotype. ♀, China: Sichuan Prov., Luding County, Tianba, Mujiaogou, 2124 m, 8.x.2014, coll. Qikun Bai, Zhiwei Qiu and Xinran Li.

Paratypes. 1♂, 3♀, same data as holotype.

Measurements

Male and female – pronotum, length × width: 5.5 × 8.0 mm; body length: 24.5 mm.

Description

Tergite VII with anterior margin slightly truncate, posterior margin truncate (Fig. 13*D*). Sternum VII produced at apex, posterior margin truncate (Fig. 13*C*). Tergite X rounded at apex; paraprocts (pp.) developed, triangular, with apices not extending to the posterior margin of Tergite X (Fig. 13*A*).

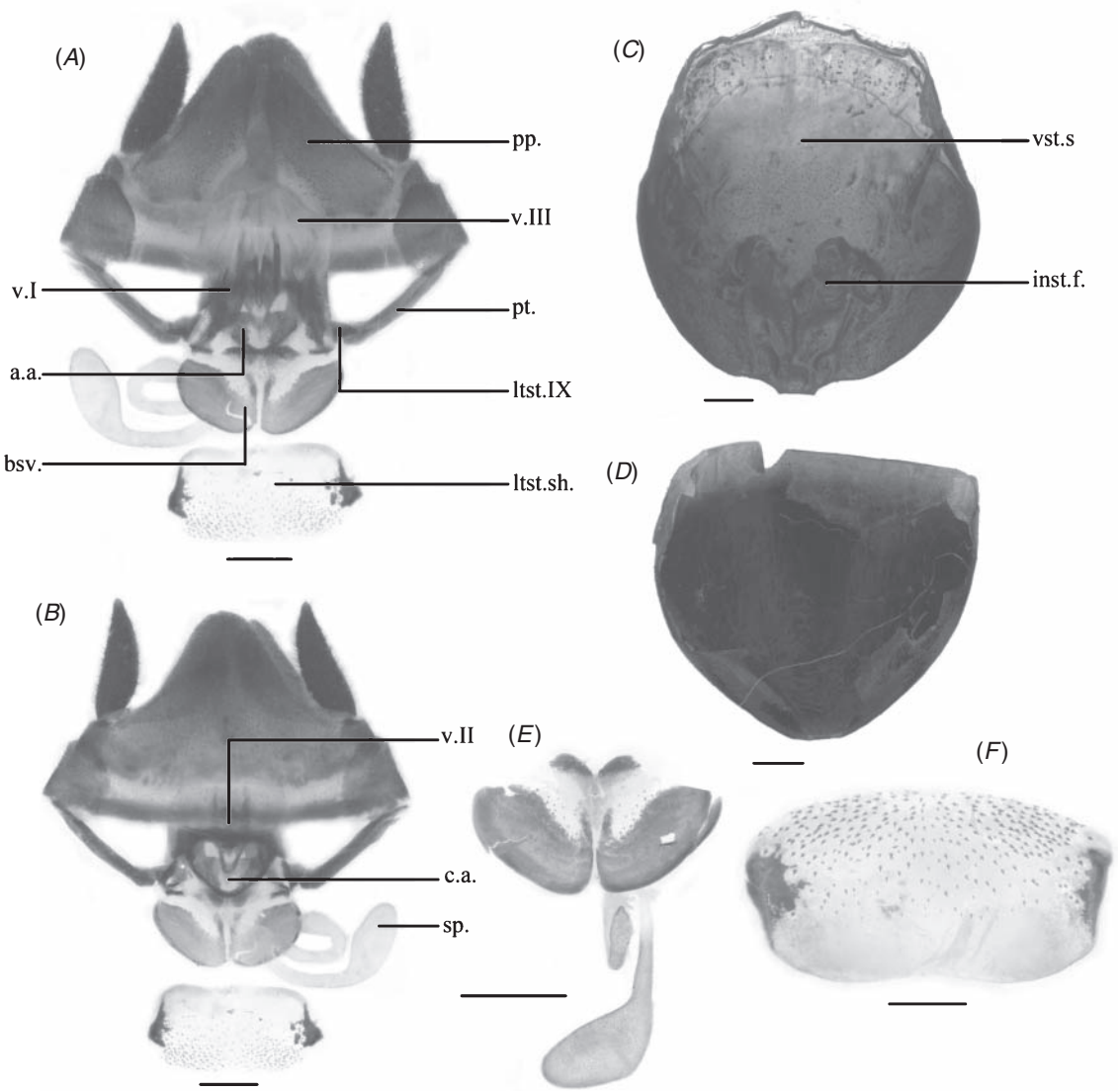

Fig. 10. *Cryptocercus luanchuanensis*, sp. nov.: (*A*) supraanal plate, ventral view; (*B*) supraanal plate, dorsal view; (*C*) subgenital plate, dorsal view; (*D*) Tergite VII, dorsal view; (*E*) basivalvula and spermatheca, ventral view; (*F*) laterosternal shelf, dorsal view. Scale bars: 1.0 mm.

Female genitalia

Basivalvulae (bsv.) well developed and divided into two symmetrical parts; basivalvulae with anterior and posterior margins clearly delimited, posterior margins dark brown, anterior area wide and dark brown (Fig. 13*E*). Spermatheca sitting behind the basivalvulae and with a large and oblong apical ampulla, and an oblong basal ampulla on a short duct. Laterosternal shelf (ltst.sh.) large and translucent, nearly oblong and narrow, brown at middle, with dense spinules at apical half (Fig. 13*F*).

Remarks

All nine new species of *Cryptocercus* were extremely similar in external morphology. We chose five standard characters of female genitalia that have been used to distinguish species in previous studies (Grandcolas 2000; Grandcolas *et al*. 2001, 2005; Aldrich *et al*. 2004; Wang *et al*. 2015). Most species can be identified on the basis of these characters, e.g. interspecific character variation of characters between *C. chengkouensis*, sp. nov. and *C. changbaiensis*, sp. nov. (Table 2): *C. chengkouensis*, sp. nov. has a distinctive prominence on the anterior area of the basivalvulae (Fig. 5*E*) but the latter does not (Fig. 6*E*); two sides of the laterosternal shelf in the former are brown (Fig. 5*F*), but not in the latter (Fig. 6*F*); the spermatheca of *C. chengkouensis*, sp. nov. is oval (Fig. 5*E*), but nearly round in the latter (Fig. 6*E*). Unfortunately, identification of similar *Cryptocercus* species using just these five characters would be challenging for a large-scale biodiversity study, because there is a considerable morphological overlap between the related species (e.g. *C. luanchuanensis* sp. nov. (Fig. 10) and *C. neixiangensis*). DNA-based tools have been shown to be a

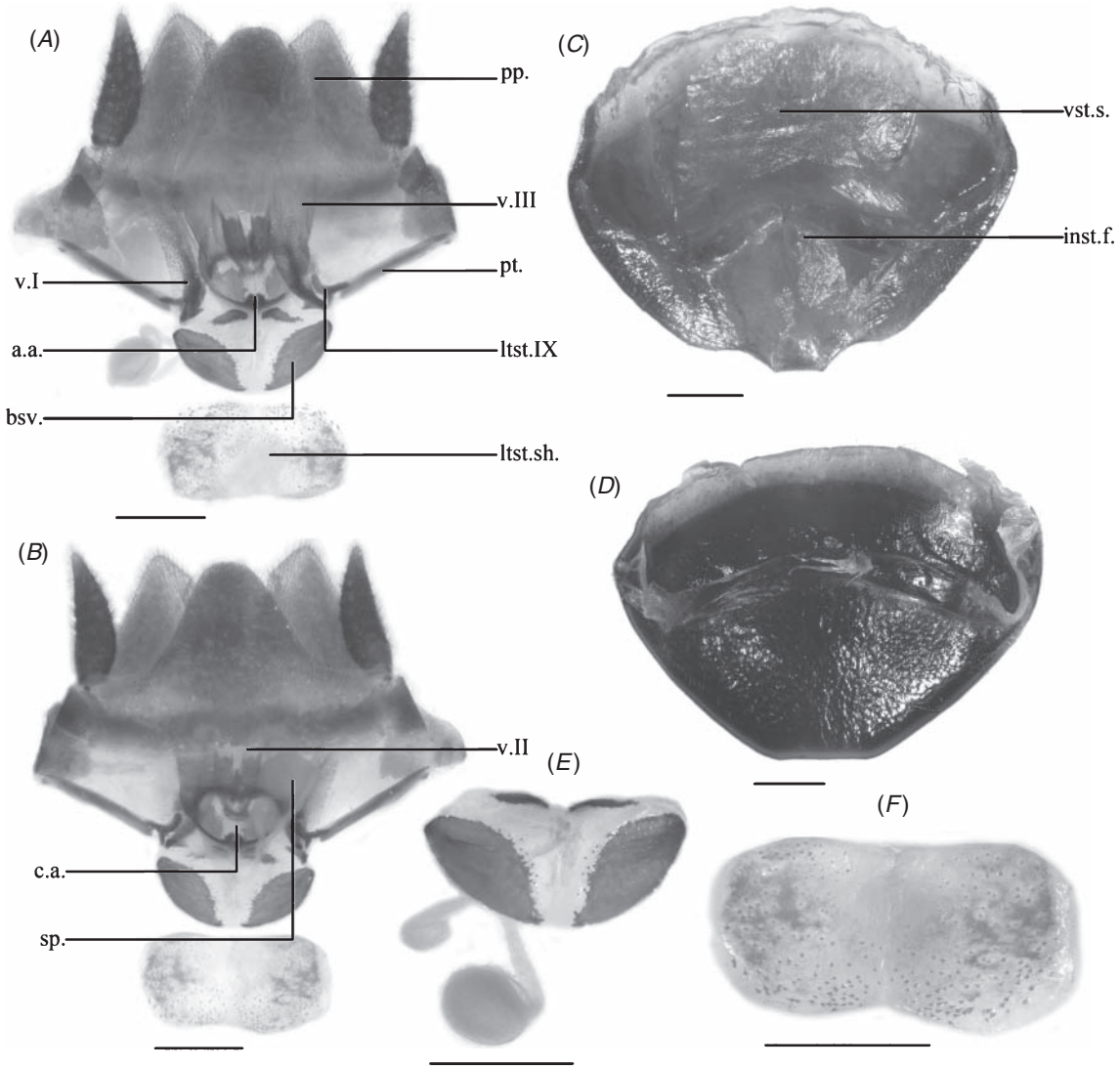

Fig. 11. *Cryptocercus laojunensis*, sp. nov.: (*A*) supraanal plate, ventral view; (*B*) supraanal plate, dorsal view; (*C*) subgenital plate, dorsal view; (*D*) Tergite VII, dorsal view; (*E*) basivalvula and spermatheca, ventral view; (*F*) laterosternal shelf, dorsal view. Scale bars: 1.0 mm.

valuable and effective approach to identify *Cryptocercus* species (Kambhampati 1996; Burnside *et al*. 1999), so we combined DNA barcoding and morphology with chromosome number to delimit species. Until now, molecular techniques have been the most rapid and convenient approach for studying these species of woodroaches.

Discussion

Species delimitation

The nine candidate species we identified, primarily on the basis of chromosome numbers, are in addition to the 15 identified previously by Grandcolas (2000), Grandcolas *et al*. (2005), Wang *et al*. (2015), and Che *et al*. (2016). Molecular species delimitation analysis corroborated the existence of each of these species. Our results indicate that DNA-based species-delimitation methods using COI perform well for these subsocial and xylophagous cockroaches, and are likely to be of utility given the lack of defining morphological characters among males, females and nymphs of these organisms. Our study is the first attempt to delimit *Cryptocercus* species on a large scale, including males, females and nymphs.

As the genus *Cryptocercus* comprises mainly alpine cockroaches, we were able to obtain only a small number of samples from each locality. This may have contributed to the limited genetic variability within each species. Barcode gap (COI) analysis showed that the maximum intraspecific distance (0.61%) was distinctly lower than the interspecific distance (2.18–20.36%), even for those species (*C. neixiangensis* and *C. luanchuanensis*, sp. nov.) with the lowest interspecific divergence (2.18%). Hebert *et al*. (2004) proposed that the genetic divergence cutoff for species identification should be at least 10 times greater than within species. Our study (average intraspecific distance: 0.14%, average interspecific distance: 11.81%) showed that there is a distinct gap between intraspecific and interspecific distances. DNA-based analyses

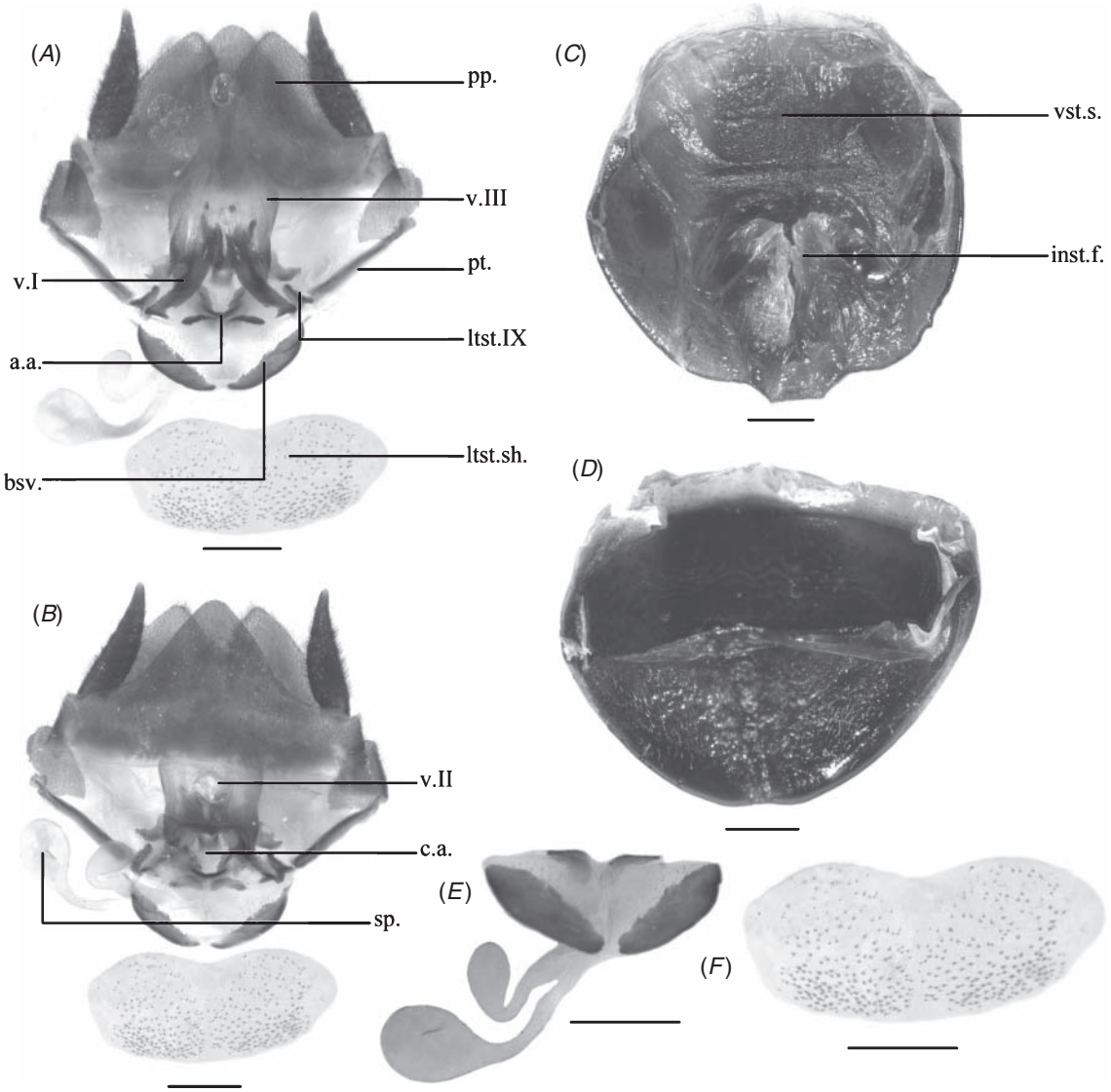

Fig. 12. *Cryptocercus banshanmenensis*, sp. nov.: (*A*) supraanal plate, ventral view; (*B*) supraanal plate, dorsal view; (*C*) subgenital plate, dorsal view; (*D*) Tergite VII, dorsal view; (*E*) basivalvula and spermatheca, ventral view; (*F*) laterosternal shelf, dorsal view. Scale bars: 1.0 mm.

resolved most *Cryptocercus* samples from Asia to a putative species. GMYC, ABGD and chromosome numbers enabled their differentiation of the two geographically proximate species *C. neixiangensis* (BTM) ($2n = 37$) and *C. luanchuanensis*, sp. nov. (LYW) ($2n = 39$) (Fig. 2) (2.18% in COI, 1% in 28S), although they had highly similar morphologies. Some other species pairs were particularly well differentiated despite being geographically proximate to each other (e.g. *C. primarius* (DCP) and *C. pingwuensis* (BSG) – 4 km apart).

Uplifting of the Qinghai–Tibetan plateau caused rich diversity of Cryptocercus in the Hengduan Mountains

To date 22 *Cryptocercus* species have been described worldwide, of which 16 are from China (Bey-Bienko 1938; Grandcolas 2000; Grandcolas *et al*. 2005; Wang *et al*. 2015; Che *et al*. 2016). Another nine new *Cryptocercus* species, mainly from the Hengduan Mountains (six species), are described in the current study. There are now 25 *Cryptocercus* species distributed in the mountain forests from 702 m (Gaolingzi, Heilongjiang Province) to 3756 m (Shikaxueshan, Yunnan Province) in China, most of which are in the Hengduan Mountains.

The Hengduan Mountains comprise a large mountainous region in south-western China with an average elevation of more than 4000 m (Spicer *et al*. 2003). Fifteen *Cryptocercus* species were discovered here at an altitude of ~3000 m. The Himalayan and Hengduan Mountains are known to encompass global biodiversity hotspots with high levels of plant and animal biodiversity and endemism (Myers *et al*. 2000; Wu *et al*. 2013; Liu *et al*. 2014). The region is thought to harbour at least 15 000 land plant species, of which more than 29% are endemic, and at least 1141 vertebrate species, of which 15% are

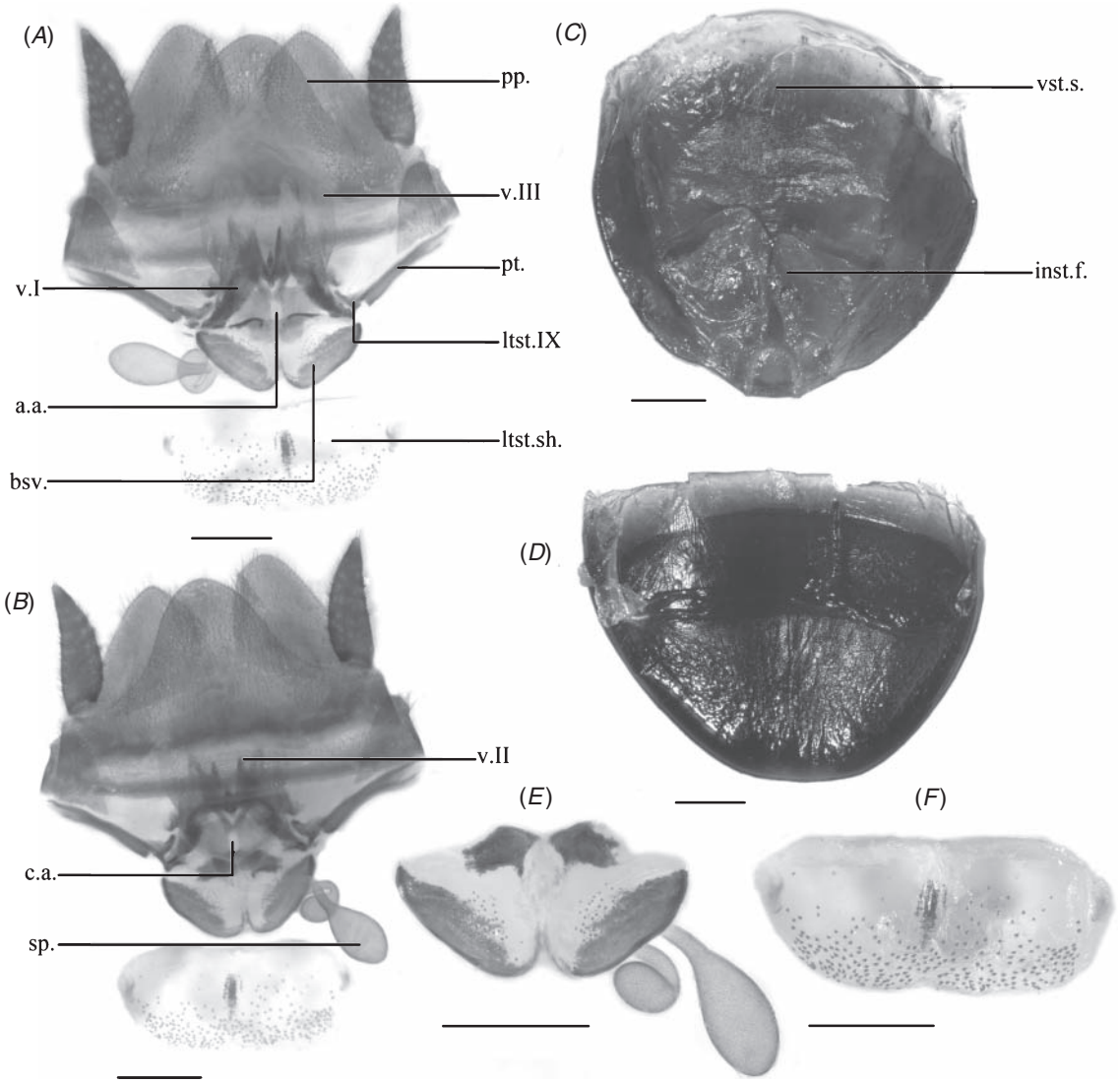

Fig. 13. *Cryptocercus tianbaensis*, sp. nov.: (*A*) supraanal plate, ventral view; (*B*) supraanal plate, dorsal view; (*C*) subgenital plate, dorsal view; (*D*) Tergite VII, dorsal view; (*E*) basivalvula and spermatheca, ventral view; (*F*) laterosternal shelf, dorsal view. Scale bars: 1.0 mm.

endemic (Myers *et al*. 2000). The rapid and extensive uplift of the Himalaya–Hengduan Mountains is considered to be the major driving force in shaping such high species diversity (Liu *et al*. 2013; Wu *et al*. 2013; Wen *et al*. 2014). The Hengduan Mountains can be considered to be one of the hotspots of *Cryptocercus* diversity in China.

Since the early Miocene, extensive uplifting of the Qinghai–Tibetan plateau occurred over at least four major periods: 25–17, 15–13, 8–7, and 3.5–1.6 million years ago (Allégre *et al*. 1984; Spicer *et al*. 2003; Royden *et al*. 2008). The *Cryptocercus* lineages in the Hengduan Mountains began to diversify 20.7–11.7 million years ago, and the most recent diversification between *C. arcuatus* (SKXS) and *C. habaensis* (HBXS) occurred ~5.82–1.58 million years ago (Che *et al*. 2016), which corresponds well with the major uplifts of the Qinghai–Tibetan plateau. This region is characterised by a series of parallel mountain ranges (Yin and Harrison 2000), but all members of *Cryptocercus* are wingless and lack the ability to migrate over long distances. The physical isolation caused by these mountain ranges is likely to have contributed to interspecific and intraspecific divergences. The localities of two close geographic species, *C. habaensis* (Fig. 14*E*) and *C. meridianus* (Fig. 14*D*), are found just 28 km apart, but they are separated by two snow mountains (Haba Snow Mountain, 5396 m; Yulong Snow Mountain, 5596 m) and one gorge (Tiger Leaping Gorge) (Fig. 14*A*). Tiger Leaping Gorge passes between the two Snow Mountains in a dramatic vertical drop of 3500 m, through which a rapid stream flows and xeric shrubland exists on both banks along the Jinsha River (Qikun Bai, pers. obs.). These natural barriers prevent gene flow among *Cryptocercus* species. Significant genetic differences (9.50% in COI) can be detected between these two species. Similarly, there is no vegetation on the

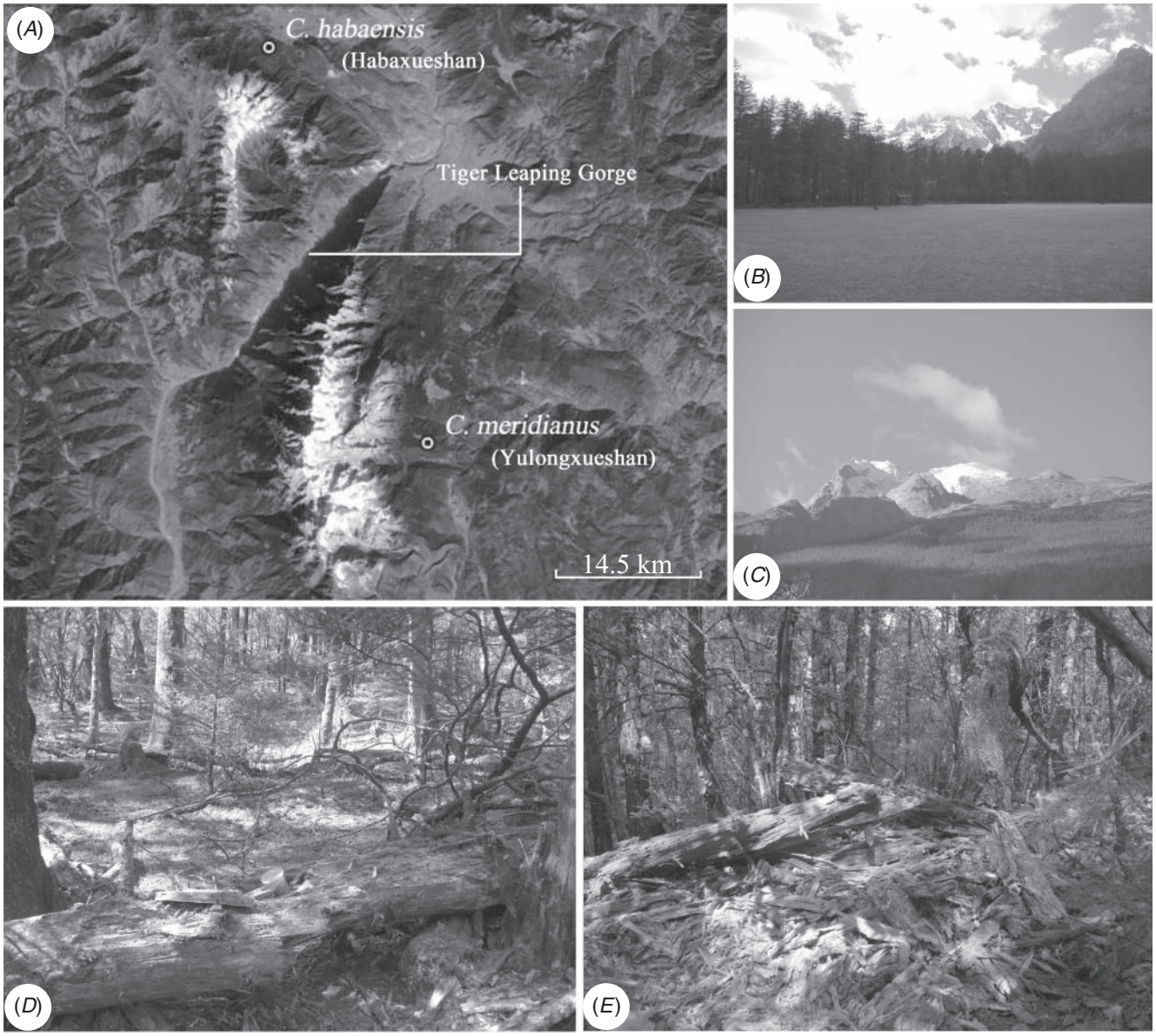

Fig. 14. Collection sites for *Cryptocercus* at Mt Habaxueshan and Mt Yulongxueshan: (*A*) the whole topographical map of Mt Habaxueshan and Mt Yulongxueshan, map data: Google, Copernicus; (*B*) photograph of Mt Yulongxueshan; (*C*) photograph of Mt Habaxueshan; (*D*) habitat of *C. meridianus*; (*E*) habitat of *C. habaensis*. All photographs by Qikun Bai.

peaks of ridges at altitudes of 4000–5000 m (Wang *et al*. 2004), which would prevent migration by *Cryptocercus* from one peak to another (Fig. 14*B*, 1*C*).

Compared with the lineages from the Hengduan Mountains (2124–3756 m, average 2986 m), the lineages from the Qin-Daba Mountains (1470–2600 m, average 1814 m) and Manchuria (702–1199 m, average 935 m) occur at lower elevations. Relatively poor *Cryptocercus* diversity has been found in these two regions (Qin-Daba Mountains lineages: 7 species; Manchuria lineages: 2 species). Manchuria is a large north-eastern Asian geographic region of ~130 $\times$ 10^6 km^2 which mostly consists of vast plains (Elliott 2000). *C. relictus* has been collected by us at Gaolingzi, Shuangfenglinchang, and Mudanfeng as well as from Russia (Bey-Bienko 1935) and South Korea (Park *et al*. 2004). This speices therefore appears to be widely distributed in north-eastern Asia. The relatively simple geography of this region compared with the Hengduan Mountains is likely the primary cause of the low diversity in this area, because there are no major barriers to hinder the gene flow among different populations. Changbai Mountain, the highest in the Manchuria region, is an active volcano situated on the boundary between China and North Korea, and was formed within a short period between 2.77 and 0.31 million years ago (Wan 2012; Wei *et al*. 2007). It is therefore unlikely to have influenced the evolution of *Cryptocercus* in the way that the Hengduan Mountains have.

Conclusion

Our results show that molecular methods generate species hypotheses for woodroaches that are highly consistent with those based on morphological and chromosome-based hypotheses. The DNA-based technique shows promise as a rapid, precise, independent identification approach to discriminate woodroaches of different life stages and sexes. Because of its high performance, COI can be recommended as a useful DNA barcode for *Cryptocercus*. The approaches we used may also help to increase our understanding of the rich diversity of *Cryptocercus*. The wide diversity of *Cryptocercus* in the Hengduan Mountain indicates that more detailed ecological data and multiregion populations are needed to further clarify the phylogenetic relationships within Asian *Cryptocercus*. The high endemism typically displayed by *Cryptocercus* species in China makes them particularly vulnerable to habitat destruction. Our work therefore highlights the importance of protecting the alpine forests that these taxa inhabit.

Conflicts of interest

The authors declare no conflicts of interest.

Acknowledgements

We cordially thank Yejie Lin (Sichuan Agricultural University, Yaan, Sichuan), Yan Shi, Xinran Li, Zhiwei Qiu and Lu Qiu for assistance with fieldwork. We also thank two anonymous reviewers for providing comments on an early version of the manuscript. We thank Simon Ho for advice on analysis. This study is supported by the Natural Science Foundation Project of Chongqing (cstc2016jcyjA0487) and the National Natural Sciences Foundation of China (Number 31672329).

References

Aldrich, B. T., Zolnerowich, G., and Kambhampati, S. (2004). Interspecific morphological variation in the wood-feeding cockroach, *Cryptocercus* (Dictyoptera: Cryptocercidae). *Arthropod Structure & Development* **33**, 443–451. doi:10.1016/j.asd.2004.06.005

Allégre, C. J., Courtillot, V., Tapponnier, P., Hirn, A., Mattauer, M., Coulon, C., Jaeger, J. J., Achache, J., Schärer, U., and Marcoux, J. (1984). Structure and evolution of the Himalaya–Tibet orogenic belt. *Nature* **307**, 17–22. doi:10.1038/307017a0

Bey-Bienko, G. (1935). Descriptions of six new species of Palearctic Blattodea. *Konowia: Zeitschrift für systematische Insektenkunde* **14**, 117–134.

Bey-Bienko, G. (1938). On some new or interesting Asiatic Blattodea. *Annals & Magazine of Natural History* **1**, 230–238. doi:10.1080/00222933808526759

Burnside, C. A., Smith, P. T., and Kambhampati, S. (1999). Three new species of the wood roach, *Cryptocercus* (Blattodea: Cryptocercidae), from the eastern United States. *Journal of the Kansas Entomological Society* **72**, 361–378.

Cameron, S. L., Lo, N., Bourguignon, T., Svenson, G. J., and Evans, T. A. (2012). A mitochondrial genome phylogeny of termites (Blattodea: Termitoidae): robust support for interfamilial relationships and molecular synapomorphies define major clades. *Molecular Phylogenetics and Evolution* **65**, 163–173. doi:10.1016/j.ympev.2012.05.034

Caterino, M. S., Cho, S., and Sperling, F. A. (2000). The current state of insect molecular systematics: a thriving Tower of Babel. *Annual Review of Entomology* **45**, 1–54. doi:10.1146/annurev.ento.45.1.1

Che, Y. L., Wang, D., Shi, Y., Du, X. H., Zhao, Y. Q., Lo, N., and Wang, Z. Q. (2016). A global molecular phylogeny and timescale of evolution for *Cryptocercus* woodroaches. *Molecular Phylogenetics Evolution* **98**, 201–209.

Che, Y. L., Gui, S. H., Lo, N., Ritchie, A., and Wang, Z. Q. (2017). Species delimitation and phylogenetic relationships in ectobiid cockroaches (Dictyoptera, Blattodea) from China. *PLoS One* **12**, e0169006. doi:10.1371/journal.pone.0169006

Desalle, R. (2006). Species discovery versus species identification in DNA barcoding efforts: response to Rubinoff. *Conservation Biology* **20**, 1545–1547. doi:10.1111/j.1523-1739.2006.00543.x

Drummond, A. J., and Rambaut, A. (2007). BEAST: Bayesian evolutionary analysis by sampling trees. *BMC Evolutionary Biology* **7**, 214. doi:10.1186/1471-2148-7-214

Edgar, R. C. (2004). MUSCLE: multiple sequence alignment with high accuracy and high throughput. *Nucleic Acids Research* **32**, 1792–1797. doi:10.1093/nar/gkh340

Elliott, M. C. (2000). The limits of Tartary: Manchuria in imperial and national geographies. *The Journal of Asian Studies* **59**, 603–646. doi:10.2307/2658945

Evangelista, D. A., Bourne, G., and Ware, J. L. (2014). Species richness estimates of Blattodea s.s. (Insecta: Dictyoptera) from northern Guyana vary depending upon methods of species delimitation. *Systematic Entomology* **39**, 150–158. doi:10.1111/syen.12043

Everaerts, C., Maekawa, K., Farine, J. P., Shimada, K., Luykx, P., Brossut, R., and Nalepa, C. A. (2008). The *Cryptocercus punctulatus* species complex (Dictyoptera: Cryptocercidae) in the eastern United States: comparison of cuticular hydrocarbons, chromosome number, and DNA sequences. *Molecular Phylogenetics and Evolution* **47**, 950–959. doi:10.1016/j.ympev.2008.03.011

Ezard, T., Fujisawa, T., and Barraclough, T. (2009). Splits: species' limits by threshold statistics. R package version 1.0–11/r29.

Fujisawa, T., and Barraclough, T. G. (2013). Delimiting species using single-locus data and the Generalized Mixed Yule Coalescent approach: a revised method and evaluation on simulated data sets. *Systematic Biology* **62**, 707–724. doi:10.1093/sysbio/syt033

Grandcolas, P. (2000). Cryptocercus matilei n. sp., du Sichuan de Chine [Dictyoptera, Blattaria, Polyphaginae]. *Revue Francaise d'Entomologie* **22**, 223–226.

Grandcolas, P., Park, Y. C., Choe, J. C., Piulachs, M. D., Bellés, X., D'Haese, C., Farine, J. P., Brossut, R., and Farine, J. P. (2001). What does *Cryptocercus kyebangensis*, n. sp. (Dictyoptera, Blattaria, Polyphagidae) from Korea reveal about *Cryptocercus* evolution? A study in morphology, molecular phylogeny, and chemistry of tergal glands. *Proceedings. Academy of Natural Sciences of Philadelphia* **151**, 61–79. doi:10.1635/0097-3157(2001)151[0061:WDCKNS]2.0.CO;2

Grandcolas, P., Legendre, F., Park, Y. C., Belles, X., Murienne, J., and Pellens, R. (2005). The genus *Cryptocercus* in East Asia: distribution and new species (Insecta, Dictyoptera, Blattaria, Polyphagidae). *Zoosystema* **27**, 725–732.

Hausmann, A., Haszprunar, G., and Hebert, P. D. N. (2011). DNA barcoding the geometrid fauna of Bavaria (Lepidoptera): successes, surprises, and questions. *PLoS One* **6**, e17134. doi:10.1371/journal.pone.0017134

Hebert, P. D. N., Cywinska, A., Ball, S. L., and deWaard, J. R. (2003). Biological identifications through DNA barcodes. *Proceedings of the Royal Society of London. Series B, Biological Sciences* **270**, 313–321. doi:10.1098/rspb.2002.2218

Hebert, P. D. N., Stoeckle, M. Y., Zemlak, T. S., and Francis, C. M. (2004). Identification of birds through DNA barcodes. *PLoS Biology* **2**, e312. doi:10.1371/journal.pbio.0020312

Inward, D. J., Vogler, A. P., and Eggleton, P. (2007). A comprehensive phylogenetic analysis of termites (Isoptera) illuminates key aspects of their evolutionary biology. *Molecular Phylogenetics and Evolution* **44**, 953–967. doi:10.1016/j.ympev.2007.05.014

Kambhampati, S. (1996). Phylogenetic relationship among cockroach families inferred from mitochondrial 12S rRNA gene sequence. *Systematic Entomology* **21**, 89–98.

Kambhampati, S., Luykx, P., and Nalepa, C. A. (1996). Evidence for sibling species in *Cryptocercus punctulatus*, the wood roach, from variation in mitochondrial DNA and karyotype. *Heredity* **76**, 1–12.

Kimura, M. (1980). A simple method for estimating evolutionary rates of base substitutions through comparative studies of nucleotide sequences. *Journal of Molecular Evolution* **16**, 111–120. doi:10.1007/BF01731581

Klass, K. D., and Meier, R. (2006). A phylogenetic analysis of Dictyoptera (Insecta) based on morphological characters. *Entomologische Abhandlungen* **63**, 3–50.

Knebelsberger, T., and Miller, M. A. (2007). Revision and phylogeny of the *subaptera*-group of *Phyllodromica* (Blattoptera: Blattellidae: Ectobiinae), including a parthenogenetic species and the evaluation of COI sequences for species identification (DNA barcoding). *Zootaxa* **1522**, 1–68.

Lanfear, R., Calcott, B., Ho, S. Y., and Guindon, S. (2012). Partitionfinder: combined selection of partitioning schemes and substitution models for phylogenetic analyses. *Molecular Biology and Evolution* **29**, 1695–1701. doi:10.1093/molbev/mss020

Li, Y., Wang, Z. Q., and Che, Y. L. (2013). A comparative study of the oothecae and female genitalia of seven species of Blattodea. *Acta Zootaxonomica Sinica* **38**, 16–26.

Liu, J., Moller, M., Provan, J., Gao, L. M., Poudel, R. C., and Li, D. Z. (2013). Geological and ecological factors drive cryptic speciation of yews in a biodiversity hotspot. *New Phytologist* **199**, 1093–1108. doi:10.1111/nph.12336

Liu, J. Q., Duan, Y. W., Hao, G., Ge, X. J., and Sun, H. (2014). Evolutionary history and underlying adaptation of alpine plants on the Qinghai–Tibet Plateau. *Journal of Systematics and Evolution* **52**, 241–249. doi:10.1111/jse.12094

Lo, N., Tokuda, G., Watanabe, H., Rose, H., Slaytor, M., Maekawa, K., Bandi, C., and Noda, H. (2000). Evidence from multiple gene sequences indicates that termites evolved from wood-feeding cockroaches. *Current Biology* **10**, 801–804. doi:10.1016/S0960-9822(00)00561-3

Lo, N., Luykx, P., Santoni, R., Beninati, T., Bandi, C., Casiraghi, M., Wenhua, L., Zakharov, E. V., and Nalepa, C. A. (2006). Molecular phylogeny of *Cryptocercus* wood-roaches based on mitochondrial COII and 16S sequences, and chromosome numbers in Palearctic representatives. *Zoological Science* **23**, 393–398. doi:10.2108/zsj.23.393

Lo, N., Beninati, T., Stone, F., Walker, J., and Sacchi, L. (2007). Cockroaches that lack *Blattabacterium* endosymbionts: the phylogenetically divergent genus *Nocticola*. *Biology Letters* **3**, 327–330. doi:10.1098/rsbl.2006.0614

Luykx, P. (1983). XO:XX sex chromosomes and Robertsonian variation in the autosomes of the wood-roach *Cryptocercus punctulatus* (Dictyoptera: Blattaria: Cryptocercidae). *Annals of the Entomological Society of America* **76**, 518–522. doi:10.1093/aesa/76.3.518

McKittrick, F. A. (1964). Evolutionary studies of cockroaches. Cornell Univ. Agric. Exp. Sta., N. Y. State Coll. Of Agric. Mem. 389, 197 pp., Pls. 1–64.

Monaghan, M. T., Wild, R., Elliot, M., Fujisawa, T., Balke, M., Inward, D. J., Lees, D. C., Ranaivosolo, R., Eggleton, P., Barraclough, T. G., and Vogler, A. P. (2009). Accelerated species inventory on Madagascar using coalescent-based models of species delineation. *Systematic Biology* **58**, 298–311. doi:10.1093/sysbio/syp027

Myers, N., Mittermeier, R. A., Mittermeier, C. G., Da Fonseca, G. A., and Kent, J. (2000). Biodiversity hotspots for conservation priorities. *Nature* **403**, 853–858. doi:10.1038/35002501

Nalepa, C. A. (1984). Colony composition, protozoan transfer and some life history characteristics of the woodroach *Cryptocercus punctulatus* Scudder (Dictyoptera: Cryptocercidae). *Behavioral Ecology and Sociobiology* **14**, 273–279. doi:10.1007/BF00299498

Nalepa, C., Byers, G., Bandi, C., and Sironi, M. (1997). Description of *Cryptocercus clevelandi* (Dictyoptera: Cryptocercidae) from the northwestern United States, molecular analysis of bacterial symbionts in its fat body, and notes on biology, distribution, and biogeography. *Annals of the Entomological Society of America* **90**, 416–424. doi:10.1093/aesa/90.4.416

Park, Y. C., and Choe, J. C. (2003). Life history and population dynamics of Korean woodroach (*Cryptocercus kyebangensis*) populations. *Korean Journal of Biological Sciences* **7**, 111–117. doi:10.1080/12265071.2003.9647691

Park, Y. C., Maekawa, K., Matsumoto, T., Santoni, R., and Choe, J. C. (2004). Molecular phylogeny and biogeography of the Korean woodroaches *Cryptocercus* spp. *Molecular Phylogenetics and Evolution* **30**, 450–464. doi:10.1016/S1055-7903(03)00220-3

Pons, J., Barraclough, T., Gomez-Zurita, J., Cardoso, A., Duran, D., Hazell, S., Kamoun, S., Sumlin, W., and Vogler, A. (2006). Sequence-based species delimitation for the DNA taxonomy of undescribed insects. *Systematic Biology* **55**, 595–609. doi:10.1080/10635150600852011

Puillandre, N., Lambert, A., Brouillet, S., and Achaz, G. (2012). ABGD, Automatic Barcode Gap Discovery for primary species delimitation. *Molecular Ecology* **21**, 1864–1877. doi:10.1111/j.1365-294X.2011.05239.x

R Core Team (2013) 'R: a Language and Environment for Statistical Computing.' (R Foundation for Statistical Computing: Vienna, Austria.)

Ronquist, F., Teslenko, M., van der Mark, P., Ayres, D. L., Darling, A., Hohna, S., Larget, B., Liu, L., Suchard, M. A., and Huelsenbeck, J. P. (2012). MrBayes 3.2: efficient Bayesian phylogenetic inference and model choice across a large model space. *Systematic Biology* **61**, 539–542. doi:10.1093/sysbio/sys029

Royden, L. H., Burchfiel, B. C., and van der Hilst, R. D. (2008). The geological evolution of the Tibetan Plateau. *Science* **321**, 1054–1058. doi:10.1126/science.1155371

Scudder, S. H. (1862). Materials for a monograph of the North American Orthoptera. *Boston Journal of Natural History* **7**, 409–480. doi:10.5962/bhl.part.11211

Smith, M. A., Fisher, B. L., and Hebert, P. D. N. (2005). DNA barcoding for effective biodiversity assessment of a hyperdiverse arthropod group: the ants of Madagascar. *Philosophical Transactions of the Royal Society of London. Series B, Biological Sciences* **360**, 1825–1834. doi:10.1098/rstb.2005.1714

Spicer, R. A., Harris, N. B., Widdowson, M., Herman, A. B., Guo, S., Valdes, P. J., Wolfe, J. A., and Kelley, S. P. (2003). Constant elevation of southern Tibet over the past 15 million years. *Nature* **421**, 622–624. doi:10.1038/nature01356

Stamatakis, A., Hoover, P., and Rougemont, J. (2008). A rapid bootstrap algorithm for the RAxML web servers. *Systematic Biology* **57**, 758–771. doi:10.1080/10635150802429642

Tamura, K., Stecher, G., Peterson, D., Filipski, A., and Kumar, S. (2013). MEGA6: Molecular Evolutionary Genetics Analysis version 6.0. *Molecular Biology and Evolution* **30**, 2725–2729. doi:10.1093/molbev/mst197

Wan, F. (2012). Geological and geomorphological evolution history of Changbai Mountain of Jilin Province. *Jilin Geology* **31**, 21–23.

Wang, X., Zhang, L., and Fang, J. (2004). Geographical differences in alpine timberline and its climatic interpretation in China. *Acta Geographica Sinica* **59**, 871–879.

Wang, Z. Q., Li, Y., Che, Y. L., and Wang, J. J. (2015). The wood-feeding genus *Cryptocercus* (Blattodea: Cryptocercidae), with description of two new species based on female genitalia. *The Florida Entomologist* **98**, 260–271. doi:10.1653/024.098.0143

Ware, J. L., Litman, J., Klass, K. D., and Spearman, L. A. (2008). Relationships among the major lineages of Dictyoptera: the effect of outgroup selection on dictyopteran tree topology. *Systematic Entomology* **33**, 429–450. doi:10.1111/j.1365-3113.2008.00424.x

Wei, H. Q., Wang, Y., Jin, J. Y., Gao, L., Yun, S. H., and Jin, B. (2007). Timescale and evolution of the intracontinental Tianchi volcanic shield

and ignimbrite-forming eruption, Changbaishan, Northeast China. *Lithos* **96**, 315–324.

Wen, J., Zhang, J. Q., Nie, Z. L., Zhong, Y., and Sun, H. (2014). Evolutionary diversifications of plants on the Qinghai–Tibetan Plateau. *Frontiers in Genetics* **5**, 4. doi:10.3389/fgene.2014.00004

Wu, Y., Colwell, R. K., Rahbek, C., Zhang, C., Quan, Q., Wang, C., Lei, F., and Burns, K. C. (2013). Explaining the species richness of birds along a subtropical elevational gradient in the Hengduan Mountains. *Journal of Biogeography* **40**, 2310–2323. doi:10.1111/jbi.12177

Yin, A., and Harrison, T. M. (2000). Geologic evolution of the Himalayan-Tibetan Orogen. *Annual Review of Earth and Planetary Sciences* **28**, 211–280. doi:10.1146/annurev.earth.28.1.211

Handling editor: Gonzalo Giribet